A simple method to modulate the selectivity of aryl azide photolysis using cucurbit[8]uril

Xujun Qiu,*[a] Qianyu Cai,[a] Eric Pohl,[b] André Jung,[c] Haopu Su,[a] Olaf Fuhr,[d, e] Ute Schepers,[a, b] and Stefan Bräse*[a, c]

[a] Institute of Organic Chemistry (IOC), Karlsruhe Institute of Technology (KIT), Kaiserstraße 12, 76131 Karlsruhe, Germany. E-mail: xujun.qiu@kit.edu, braese@kit.edu.

[b] Institute of Functional Interfaces (IFG), Karlsruhe Institute of Technology (KIT), Kaiserstraße 12, 76131 Karlsruhe, Germany.

[c] Institute of Biological and Chemical Systems – Functional Molecular Systems (IBCS-FMS), Karlsruhe Institute of Technology (KIT), Kaiserstraße 12, 76131 Karlsruhe, Germany.

[d] Institute of Nanotechnology (INT), Karlsruhe Institute of Technology (KIT), Kaiserstraße 12, 76131 Karlsruhe, Germany.

[e] Karlsruhe Nano Micro Facility (KNMFi), Karlsruhe Institute of Technology (KIT), Kaiserstraße 12, 76131 Karlsruhe, Germany.

* Corresponding author

Table of Contents

1. General Remarks

Materials and Methods

The starting materials, solvents, and reagents were purchased from ABCR, ACROS, ALFA AESAR, APOLLO SCIENTIFIC, CARBOLUTION, CHEMPUR, FLUKA, FLUOROCHEM, MERCK, RIEDEL-DE HAËN, SIGMA ALDRICH, STREM, TCI, or THERMO FISHER SCIENTIFIC and used without further purification unless stated otherwise.

Solvents of technical quality were purified by distillation or with the solvent purification system MB SPS5 (acetonitrile, dichloromethane, diethyl ether) from MBRAUN. Solvents of *p.a.* quality were purchased from ACROS, FISHER SCIENTIFIC, SIGMA ALDRICH, Roth, or RIEDEL-DE HAËN and were used without further purification.

Flat-bottom crimp neck vials from ChromaGlobe with aluminum crimp caps were used for certain reactions.

Solvents were evaporated under reduced pressure at 45 °C using a rotary evaporator. For solvent mixtures, each solvent was measured volumetrically.

Flash column chromatography was performed using MERCK silica 60 (0.040 × 0.063 mm, 230–400 mesh ASTM) and quartz sand (glowed and purified with hydrochloric acid).

Reaction Monitoring

All reactions were monitored by thin-layer chromatography (TLC) using silica-coated aluminum plates (MERCK, silica 60, F254). UV active compounds were detected with a UV lamp at 254 nm and 366 nm excitation.

GC-MS (gas chromatography-mass spectrometry) measurements were performed on an AGILENT TECHNOLOGIES model 6890N (electron impact ionization), equipped with an AGILENT 19091S-433 column (5% phenyl methyl siloxane, 30 m, 0.25 µm) and a 5975B VL MSD detector with a turbopump. Helium was used as a carrier gas.

Nuclear Magnetic Resonance Spectroscopy (NMR)

NMR spectra were recorded on a BRUKER Avance 500 NMR instrument at 500 MHz for ^{1}H NMR and 126 MHz for ^{13}C NMR. The NMR spectra were recorded at room temperature in deuterated solvents acquired from EURISOTOP, SIGMA ALDRICH, or DEUTERO.

Infrared Spectroscopy (IR)

The infrared spectra were recorded with a BRUKER, Alpha P instrument. All samples were measured by attenuated total reflection (ATR). The positions of the absorption bands are given in wavenumbers $\tilde{\nu}$ in cm^{-1} and were measured in the range from 3600 cm^{-1} to 500 cm^{-1}.

Characterization of the absorption bands was done in dependence of the absorption strength with the following abbreviations: vs (very strong, 0−9%), s (strong, 10−39%), m (medium, 40−69%), w (weak, 70−89%), vw (very weak, 90−100%).

Mass Spectrometry (MS)

APCI (atmospheric pressure chemical ionization) and ESI (electrospray ionization) experiments were recorded on a Q-Exactive (Orbitrap) mass spectrometer (THERMO FISHER SCIENTIFIC, San Jose, CA, USA) equipped with a HESI II probe to record high resolution. The tolerated error is ±5 ppm of the molecular mass. The spectra were interpreted by molecular peaks $[M]^+$, or peaks of protonated molecules $[M+H]^+$ and characteristic fragment peaks and indicated with their mass-to-charge ratio (*m/z*) and intensity in percent, relative to the base peak (100%).

Photoreactions

Photoreactions were performed in a RAYONET reactor Model RPR-100 with (16) 14W light bulbs (254 nm) was used for the irradiation with UV light.

Absorption Spectroscopy

UV/Vis spectra were recorded on an Agilent Cary 100 Bio Varian UV/vis spectrometer.

Emission Spectroscopy

Emission spectra were recorded on a HORIBA SCIENTIFIC fluoromax-4 spectrofluorometer or AGILENT Cary Eclipse fluorescent spectrometer both equipped with a CZERNY-TURNER-type monochromator and a R928P PMT detector.

Preparative Reversed-Phase High-Performance Liquid Chromatography (RP-HPLC)

Preparative Reversed-Phase High-Performance Liquid Chromatography (RP-HPLC) was performed on the Puriflash™ 4125 system from Interchim. A VDSpher® C18-M-SE precolumn (10 µm, 40 x 16 mm) followed by a VDSPher® C18-M-SE separation column (10 µm, 250 x 20 mm, VDS Optilab) was used as the stationary phase. A linear gradient of acetonitrile and double distilled water supplemented with 0.1% trifluoroacetic acid (TFA) at a flow rate of 15 mL/min served as the mobile phase.

Crystallographic Information

Single crystals of $C_{26}H_{25}ClN_4O$ (**1**•H_2O), $C_{30}H_{24}F_6N_2O_4$ (**2**•$C_4HF_6O_4$), $C_{27}H_{26.5}ClN_{2.5}O$ (**3**•H_2O•½CH_3CN) were obtained by slowly evaporating aqueous solution of **1**, **2**, and **3**. A suitable crystal was selected and studied on a Stoe StadiVari diffractometer with Dectris Eiger 4M detector at 180 K using Ga-Kα radiation (λ = 1.34143 Å) generated by a Excilium Metal-Jet D2 X-ray source. Using Olex2[1] the structure was solved with the ShelXT[2] structure solution program using Intrinsic Phasing and refined with the ShelXL[3] refinement package using Least Squares minimization. Refinement was performed with anisotropic temperature factors for all non-hydrogen atoms; hydrogen atoms were calculated on idealized positions. Disordered Atoms were refined isotropically. Crystallographic data and structure refinement details are summerized in table S1, S2, and S3.

Crystallographic data for compound **1**, **2**, and **3** reported in this paper have been deposited with the Cambridge Crystallographic Data Centre as supplementary information no. CCDC-2377053, 2377054 and 2377055. Copies of the data can be obtained free of charge from https://www.ccdc.cam.ac.uk/structures/.

Density Functional Theory (DFT) calculation

The conformational analysis was carried out for **1** and **1**•CB8 complex at the B3LYP/6-31G(d,p)[4,5]/D3[6] level of theory by using the program package G16.[7] A relaxed potential energy surface (PES) scan was performed with the dihedral angle *D*(C154-C155-C161-C162) by rotating 60° in the range 0-360°. The scan for dihedral angle of C154-C155-C161-C162 started from 30° (Fig. S28), corresponding angle C10-C11-C17-C18 in **1** (Fig. S29).

2. Synthetic Procedures

4-(4'-(3-Amine) quinolin)[2.2]paracyclophane

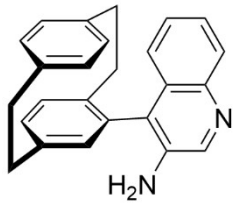

4-(4'-(3-Amine) quinolin)[2.2]paracyclophane was synthesized with the method reported from literature[8]. [2.2]Paracyclophane-4-trifluoroborate[9] (500 mg, 1.59 mmol, 1.00 equiv.), 4-bromoquinolin-3-amine[10] (426 mg, 1.91 mmol, 1.20 equiv.), palladium(II) acetate (17.9 mg, 79.6 µmol, 5.0 mol%), potassium phosphate (1.35 g, 6.37 mmol, 4.00 equiv.) and RuPhos (111 mg, 0.239 mmol, 15.0 mol%) were dissolved under argon atmosphere in toluene/water (10:1, 20 mL/2.0 mL). The mixture was heated to 80 °C for 24 h, then diluted with ethyl acetate (20 mL) and ammonium chloride (sat. aq. solution, 20 mL). The phases were separated, and the aqueous layer was extracted with ethyl acetate (2 × 20 mL). The combined organic layers were dried over sodium sulfate and the solvent was removed under reduced pressure. The crude solid was purified by flash column chromatography (silica, MeOH/DCM, 1:19) to yield the title compound 4-(4'-(3-amine) quinolin)[2.2]paracyclophane (360 mg, 1.03 mmol, 65%) as a grey solid. Due to the molecular rotation, two isomers can be observed in the NMR spectra, which cannot be integrated correspondinly.

^{1}H NMR (500 MHz, $CDCl_3$) δ = 8.70 (d, *J* = 1.4 Hz, 1H), 8.68 (d, *J* = 4.1 Hz, 4H), 8.49 (d, *J* = 7.9 Hz, 6H), 8.08 (dd, *J* = 8.3, 1.4 Hz, 2H), 8.01 – 7.92 (m, 12H), 7.72 – 7.61 (m, 6H), 7.60 – 7.42 (m, 25H), 7.41 – 7.33 (m, 7H), 7.31 – 7.23 (m, 15H), 7.17 (ddt, *J* = 8.7, 7.3, 1.3 Hz, 8H), 6.92 (d, *J* = 1.9 Hz, 5H), 6.82 (tq, *J* = 4.7, 2.8, 2.1 Hz, 8H), 6.79 (s, 3H), 6.69 (dd, *J* = 7.8, 0.8 Hz, 3H), 6.64 – 6.42 (m, 18H), 4.73 (s, 6H), 4.40 (s, 10H), 3.43 – 3.23 (m, 11H), 3.14 (dddd, *J* = 16.1, 13.6, 7.9, 4.3 Hz, 8H), 3.07 – 2.81 (m, 22H), 2.53 (ddd, *J* = 12.9, 9.7, 5.2 Hz, 3H).

^{13}C NMR (126 MHz, $CDCl_3$) δ = 144.3, 143.8, 143.4, 143.2, 143.1, 141.9, 141.1, 140.4, 140.0, 140.0, 139.8, 139.8, 139.4, 139.3, 138.5, 137.3, 136.7, 136.2, 136.0, 134.5 (d, *J* = 6.4 Hz), 134.4 (d, *J* = 3.7 Hz), 133.4, 133.0 (d, *J* = 3.2 Hz), 132.9, 132.8, 132.7 (d, *J* = 6.5 Hz), 132.3, 132.2, 132.1 – 132.0 (m), 131.4 (d, *J* = 7.1 Hz), 130.3 (d, *J* = 7.0 Hz), 129.7, 129.5, 129.1, 128.7, 128.6 (d, *J* = 2.3 Hz), 128.3 (d, *J* = 2.3 Hz), 127.8 (t, *J* = 5.2 Hz), 127.4, 127.0, 126.6, 126.1, 125.2, 125.1, 124.8 (d, *J* = 3.4 Hz), 124.6, 123.9, 123.7, 112.8, 35.7 (d, *J* = 7.5 Hz), 35.4, 35.3 (d, *J* = 2.7 Hz), 33.9, 33.3.

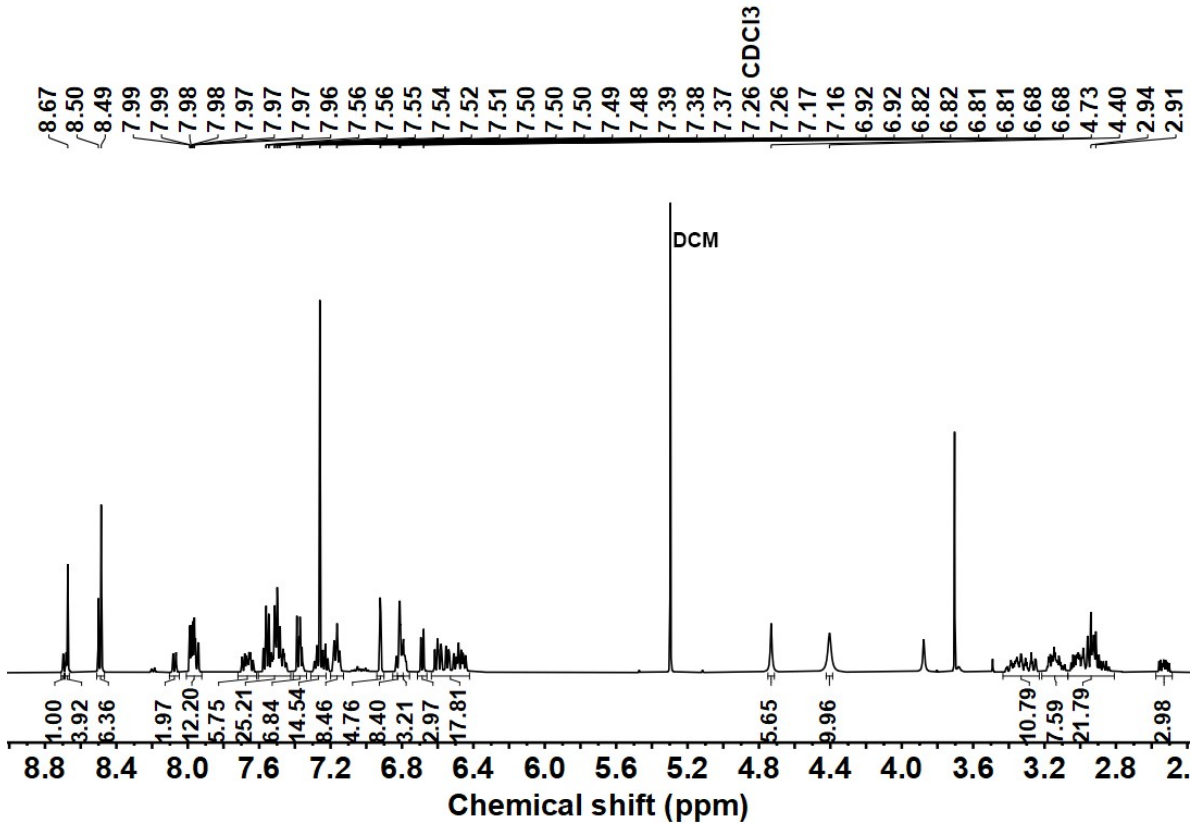

Figure S1. ^{1}H NMR –4-(4'-(3-Amine) quinolin)[2.2]paracyclophane, 500 MHz, $CDCl_3$.

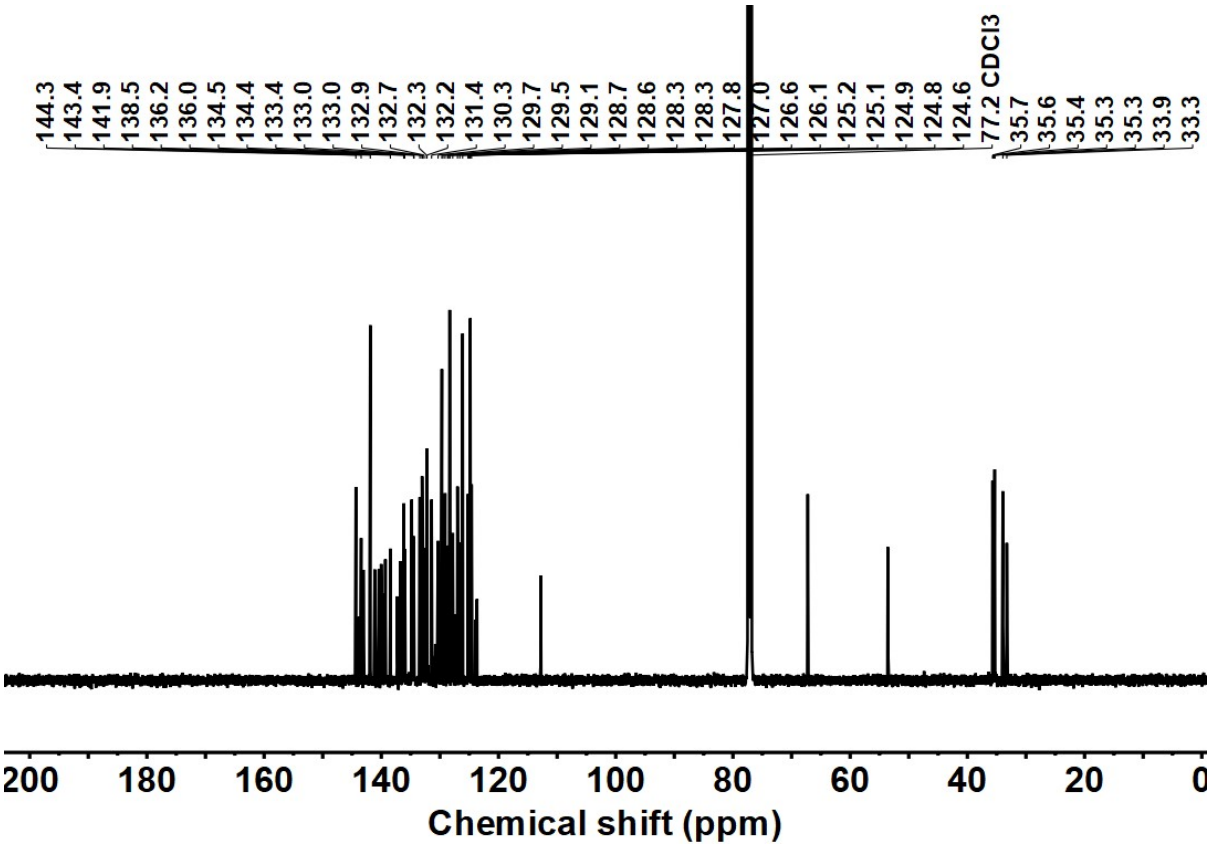

Figure S2. ^{13}C NMR –4-(4'-(3-Amine) quinolin)[2.2]paracyclophane, 126 MHz, $CDCl_3$.

ESI-MS for $[C_{25}H_{22}N_2+H]^+$: Calc. *m/z* = 351.1856, found *m/z* = 351.1852.

IR (ATR, cm^{-1}) $\tilde{\nu}$ = 3450 (vs), 3436 (vs), 3403 (vs), 3373 (vs), 3294 (vs), 3244 (vs), 3227 (vs), 3159 (vs), 3076 (vs), 3058 (vs), 3035 (vs), 3010 (vs), 2952 (vs), 2925 (vs), 2888 (vs), 2850 (vs), 2772 (s), 2765 (s), 2671 (s), 2636 (s), 2622 (s), 2612 (s), 2603 (s), 2593 (s), 2587 (s), 2580 (s), 2548 (m), 2540 (m), 2533 (m), 1621 (s), 1615 (s), 1603 (s), 1587 (s), 1567 (m), 1494 (m), 1381 (s), 1364 (m), 1341 (s) cm^{-1}.

4-(4'-(3-Azido) quinolin)[2.2]paracyclophane

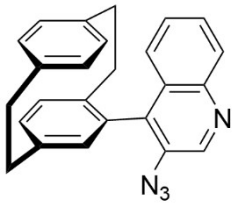

p-Toluenesulfonic acid monohydrate (163 mg, 0.86 mmol, 1.50 equiv.) was dissolved in acetonitrile/water (16/4.0 mL) at 25 °C. Once dissolved, tert-butyl nitrite (88.3 mg, 1.00 mmol, 1.50 equiv.) was added, followed by the portion-wise addition of 4-(4'-(3-amine) quinolin)[2.2]paracyclophane (0.20 g, 0.57 mmol, 1.00 equiv.). The reaction mixture was stirred for 3h at 25 °C, and then a solution of sodium azide (111 mg, 1.71 mmol, 3.00 equiv.) in water (5.0 mL) was added dropwise. The resulting reaction mass was stirred for another 3 hours at 25 °C. After the complete conversion was achieved, the reaction mixture was extracted with ethyl acetate (3 × 20 ml). The combined organic layers were dried over sodium sulfate. After the removal of the solvent, the crude solid was purified by chromatography (EtOAc: DCM=1:19) yielding 4-(4'-(3-azide) quinolin)[2.2]paracyclophane (176 mg, 0.47 mmol, 82%) as a pear color solid. Due to the molecular rotation, two isomers can be observed in the NMR spectra, which cannot be integrated correspondinly.

^{1}H NMR (500 MHz, $CDCl_3$) δ = 9.1 (s, 1H), 8.9 – 8.8 (m, 0H), 8.2 – 8.2 (m, 0H), 8.1 – 8.1 (m, 1H), 7.9 – 7.7 (m, 0H), 7.7 – 7.6 (m, 3H), 7.4 (ddd, *J* = 8.4, 6.8, 1.3 Hz, 1H), 7.0 (d, *J* = 1.8 Hz, 1H), 6.9 – 6.8 (m, 1H), 6.8 – 6.7 (m, 4H), 6.6 – 6.5 (m, 3H), 6.5 (dd, *J* = 7.8, 1.8 Hz, 1H), 6.4 (dd, *J* = 7.9, 1.9 Hz, 0H), 3.5 – 3.2 (m, 3H), 3.2 – 3.0 (m, 2H), 3.0 (dtd, *J* = 12.7, 9.7, 2.6 Hz, 3H), 2.9 – 2.8 (m, 1H), 2.7 (ddd, *J* = 13.7, 9.7, 6.0 Hz, 0H), 2.3 (ddd, *J* = 13.9, 10.2, 5.7 Hz, 1H).

^{13}C NMR (126 MHz, $CDCl_3$) δ = 147.0, 146.0, 143.4, 143.3, 140.9, 140.5, 140.0, 139.8, 139.4, 139.3, 139.2, 138.5, 135.5, 135.0 (d, *J* = 13.6 Hz), 134.8, 134.3, 133.6, 133.1, 132.7, 132.3, 132.0 (d, *J* = 2.2 Hz), 131.9, 131.7, 131.4, 130.9, 130.7 (d, *J* = 5.0 Hz), 129.8, 129.6, 128.5 (d, *J* = 3.6 Hz), 128.2, 127.8, 127.4, 126.9, 126.6, 126.5, 35.7, 35.6, 35.4, 35.3, 35.2, 34.0, 33.7.

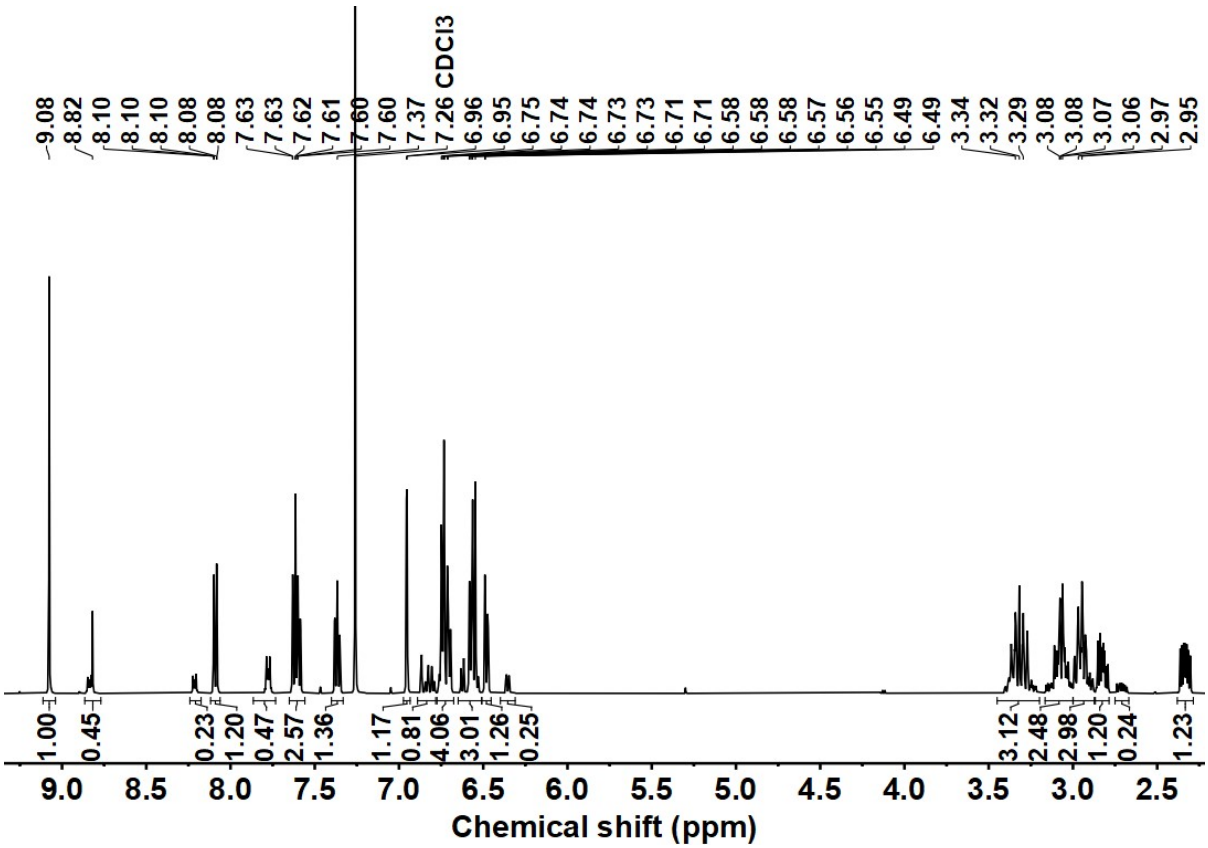

Figure S3. ^{1}H NMR –4-(4'-(3-Azido) quinolin)[2.2]paracyclophane, 500 MHz, $CDCl_3$.

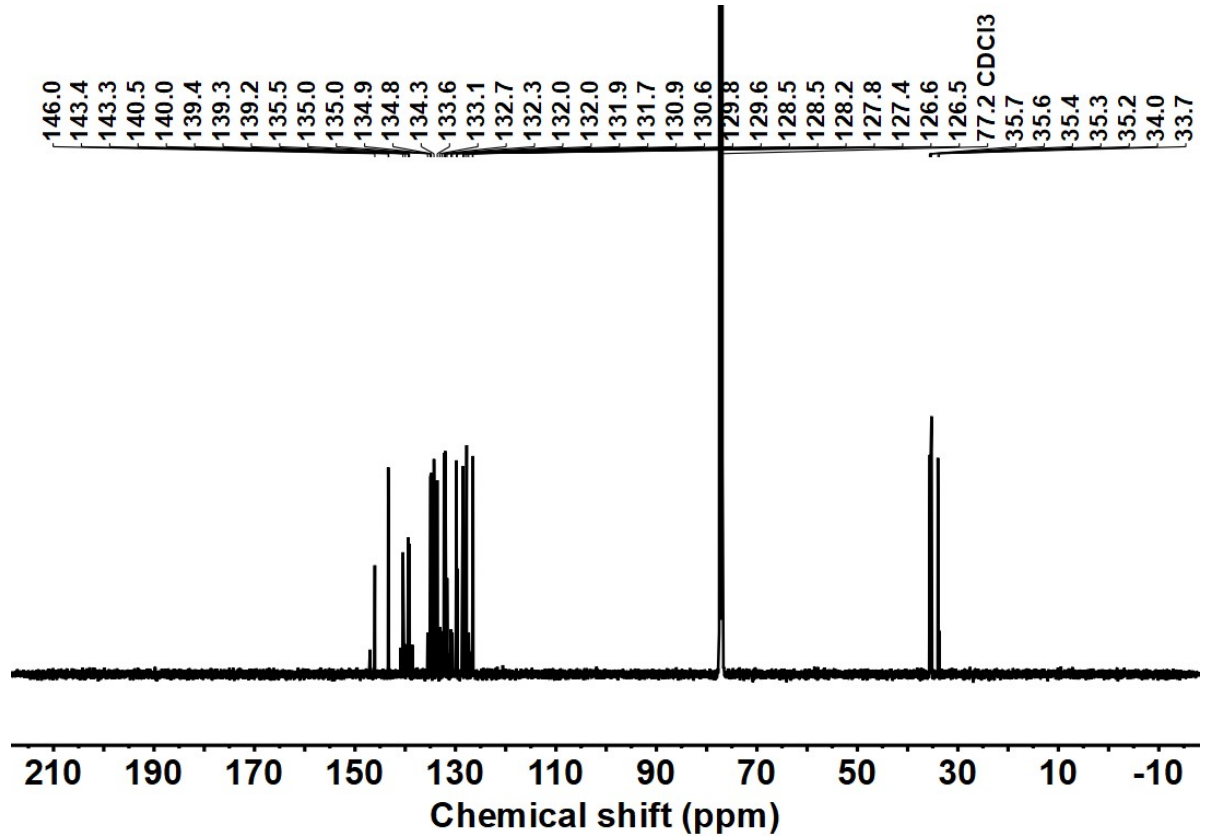

Figure S4. ^{13}C NMR –4-(4'-(3-Azido) quinolin)[2.2]paracyclophane, 126 MHz, $CDCl_3$.

ESI-MS for $[C_{25}H_{20}N_4+H]^+$: Calc. *m/z* = 377.1761, found *m/z* = 377.1759.

IR (ATR, ṽ) = 3068 (m), 3060 (m), 3023 (m), 3009 (m), 2986 (m), 2947 (s), 2925 (vs), 2886 (s), 2850 (s), 2106 (vs), 2076 (vs), 2073 (vs), 1572 (m), 1498 (m), 1315 (s), 1285 (s), 768 (m) cm^{-1}.

N-methyl-4-(4'-(3-Azido) quinolin)[2.2]paracyclophane (1)

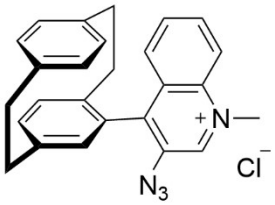

4-(4'-(3-Azido) quinolin)[2.2]paracyclophane (100 mg, 0.30 mmol, 1.00 equiv.) was dissolved in acetonitrile (10 mL), and methyl iodide (56.6 mg, 0.40 mmol, 1.50 equiv.) was added dropwise at 25 °C with stirring. The resulting reaction mixture was left 16 h at 40 °C. The precipitate was collected by filtration and washed with acetonitrile. After dissolving in 10 mL water, ammonium hexafluorophosphate (217 mg, 1.33 mmol, 5.00 equiv.) was added, which resulted in a precipitate. The precipitate was collected by filtration and washed with water, and dried. After dissolving the solid in 10 mL acetonitrile, tetrabutylammonium chloride (369 mg, 1.33 mmol, 5.00 equiv.) was added, which resulted in a precipitate. The precipitate was collected by filtration and washed with acetonitrile, acetone, and dried. The desired product N-methyl-4-(4'-(3-azido) quinolin)[2.2]paracyclophane chloride was obtained as a pear color solid (101 mg, 0.24 mmol, 89%). Due to the molecular rotation, two iosmers can be observed in the NMR spectra, which cannot be integrated corespondinly. Two isomers exsit in an approximately 3.4: 1 ratio.

^{1}H NMR (500 MHz, D_2O) δ = 9.5 (s, 1H), 9.2 (s, 0H), 9.2 – 9.1 (m, 0H), 8.4 (dd, *J* = 8.7, 1.2 Hz, 0H), 8.3 (d, *J* = 8.9 Hz, 1H), 8.2 (dddd, *J* = 22.6, 8.3, 6.9, 1.3 Hz, 1H), 8.1 (ddd, *J* = 8.8, 6.9, 1.4 Hz, 1H), 7.9 (dd, *J* = 9.1, 1.1 Hz, 1H), 7.7 (ddd, *J* = 8.5, 6.9, 0.9 Hz, 1H), 7.2 (d, *J* = 1.7 Hz, 1H), 7.0 (td, *J* = 4.0, 1.7 Hz, 1H), 6.9 (dt, *J* = 7.8, 2.0 Hz, 1H), 6.9 – 6.8 (m, 4H), 6.8 – 6.7 (m, 1H), 6.7 (dd, *J* = 7.8, 1.7 Hz, 1H), 6.6 (dd, *J* = 8.1, 1.9 Hz, 1H), 6.3 (dd, *J* = 7.9, 1.9 Hz, 0H), 4.7 (s, 3H), 4.7 (s, 1H), 3.3 (ddt, *J* = 16.3, 7.6, 4.9 Hz, 3H), 3.2 – 2.9 (m, 3H), 2.9 – 2.7 (m, 2H), 2.7 (ddd, *J* = 13.7, 10.3, 5.0 Hz, 0H), 2.2 (ddd, *J* = 13.8, 9.4, 6.4 Hz, 1H).

^{13}C NMR (126 MHz, D_2O) δ = 145.7, 144.6, 142.5, 141.9, 141.7, 141.6, 140.7, 140.3, 140.1, 139.8, 139.8 (d, *J* = 2.3 Hz), 136.5, 136.4, 136.4, 135.9, 135.6, 134.0 (d, *J* = 4.2 Hz), 133.7, 133.5, 133.4, 133.2, 132.9, 132.7, 132.4, 132.0, 131.6, 131.4 (d, *J* = 8.8 Hz), 131.1, 130.3, 130.0, 129.6, 129.4, 129.0, 128.3, 118.7, 118.1, 45.3 (d, *J* = 4.3 Hz), 36.6, 34.6, 34.5, 34.3 (d, *J* = 9.0 Hz), 33.6, 33.3.

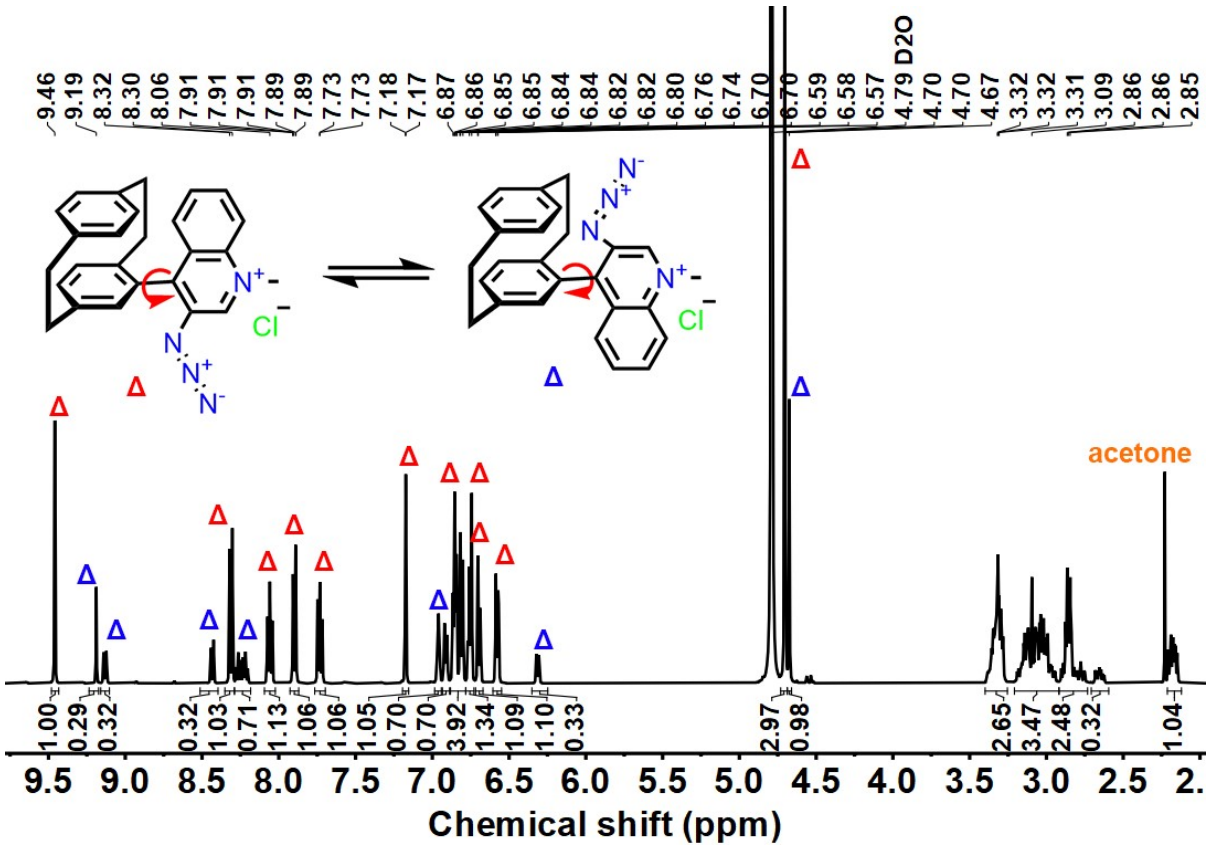

Figure S5. ^{1}H NMR – N-methyl-4-(4'-(3-Azido) quinolin)[2.2]paracyclophane (**1**), 500 MHz, $CDCl_3$.

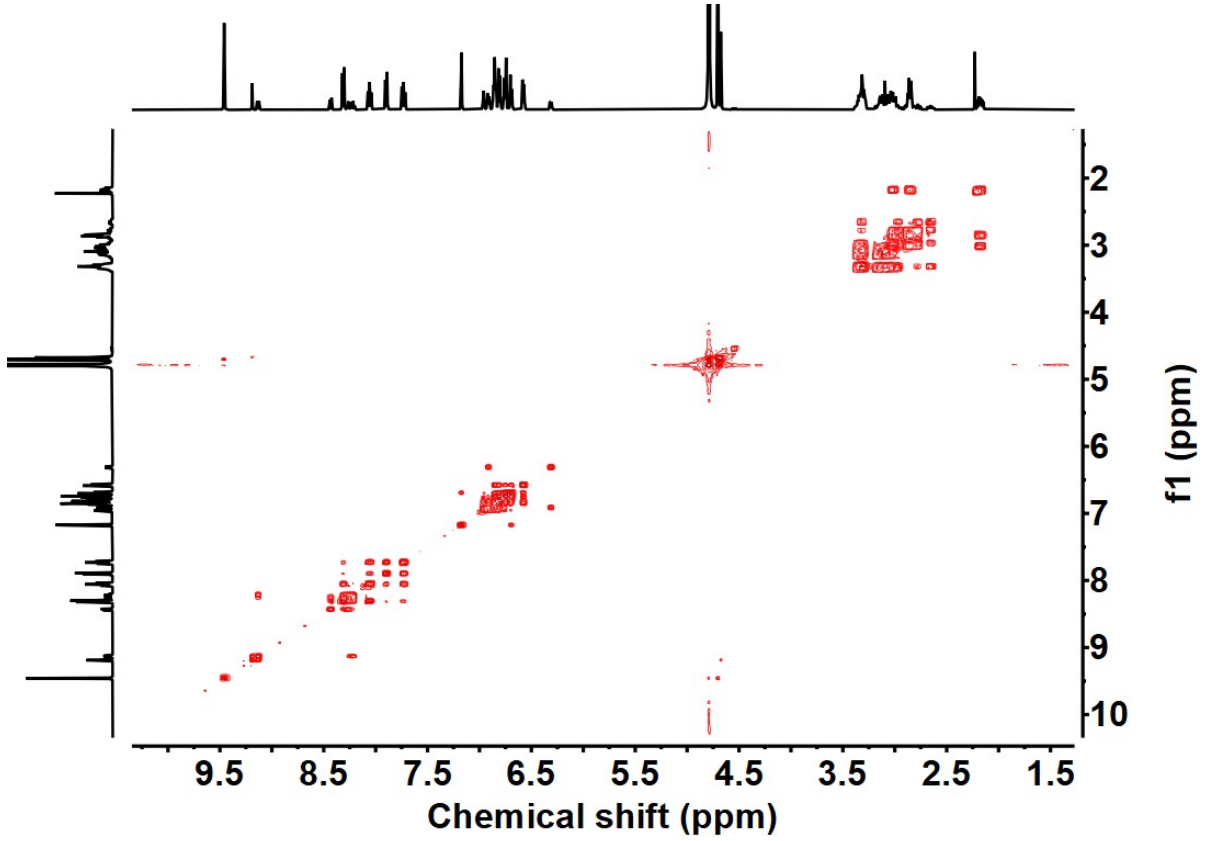

Figure S6. ^{1}H-^{1}H COSY spectra of **1**, D_2O.

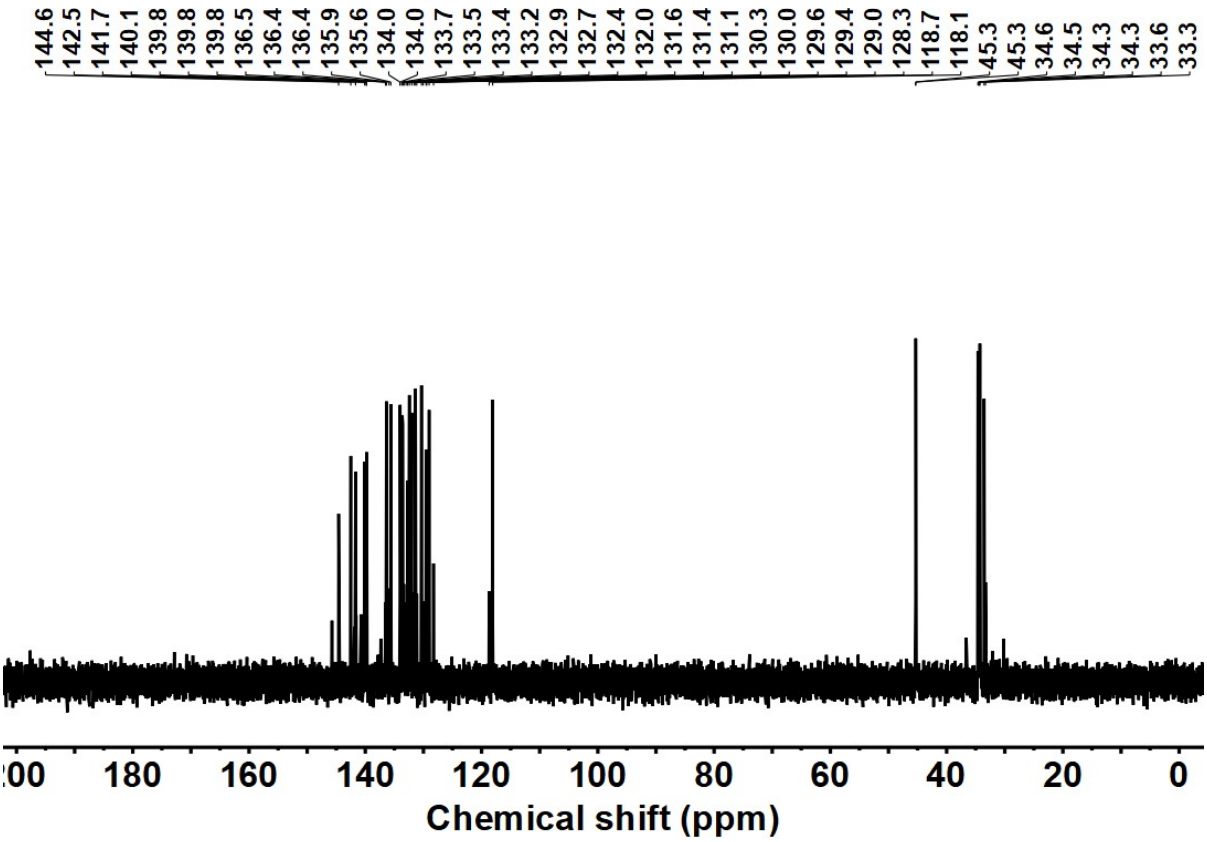

Figure S7. ^{13}C NMR – N-methyl-4-(4'-(3-Azido) quinolin)[2.2]paracyclophane (**1**), 126 MHz, $CDCl_3$.

ESI-MS for $[C_{26}H_{23}N_4]^+$: Calc. *m/z* = 391.1918, found *m/z* = 391.1907.

IR (ATR, ṽ) = 3391 (vs), 3381 (vs), 3259 (s), 3241 (s), 3233 (s), 3199 (m), 3195 (m), 3124 (m), 3121 (m), 3088 (m), 3068 (m), 3037 (m), 3022 (s), 3006 (s), 2990 (s), 2981 (s), 2923 (vs), 2893 (s), 2851 (s), 2796 (w), 2665 (w), 2119 (vs), 2025 (w), 2019 (w), 1616 (m), 1587 (w), 1567 (m), 1530 (m), 1499 (w), 1432 (w), 1424 (w), 1410 (w), 1375 (m), 1356 (s), 1311 (s), 1287 (w), 1259 (w), 771 (w), 623 (w) cm^{-1}.

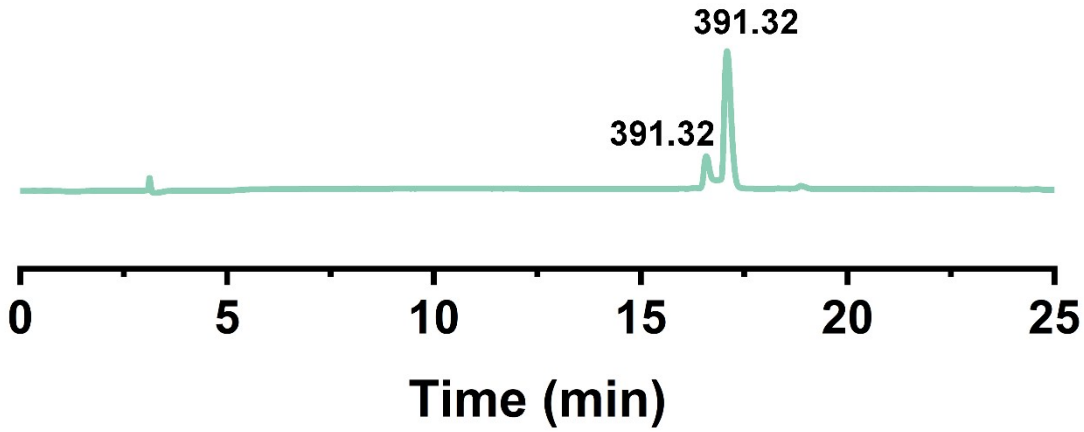

Figure S8. LC spectra of N-methyl-4-(4'-(3-Azido) quinolin)[2.2]paracyclophane (**1**).

3. Supplementary Data and Characterization

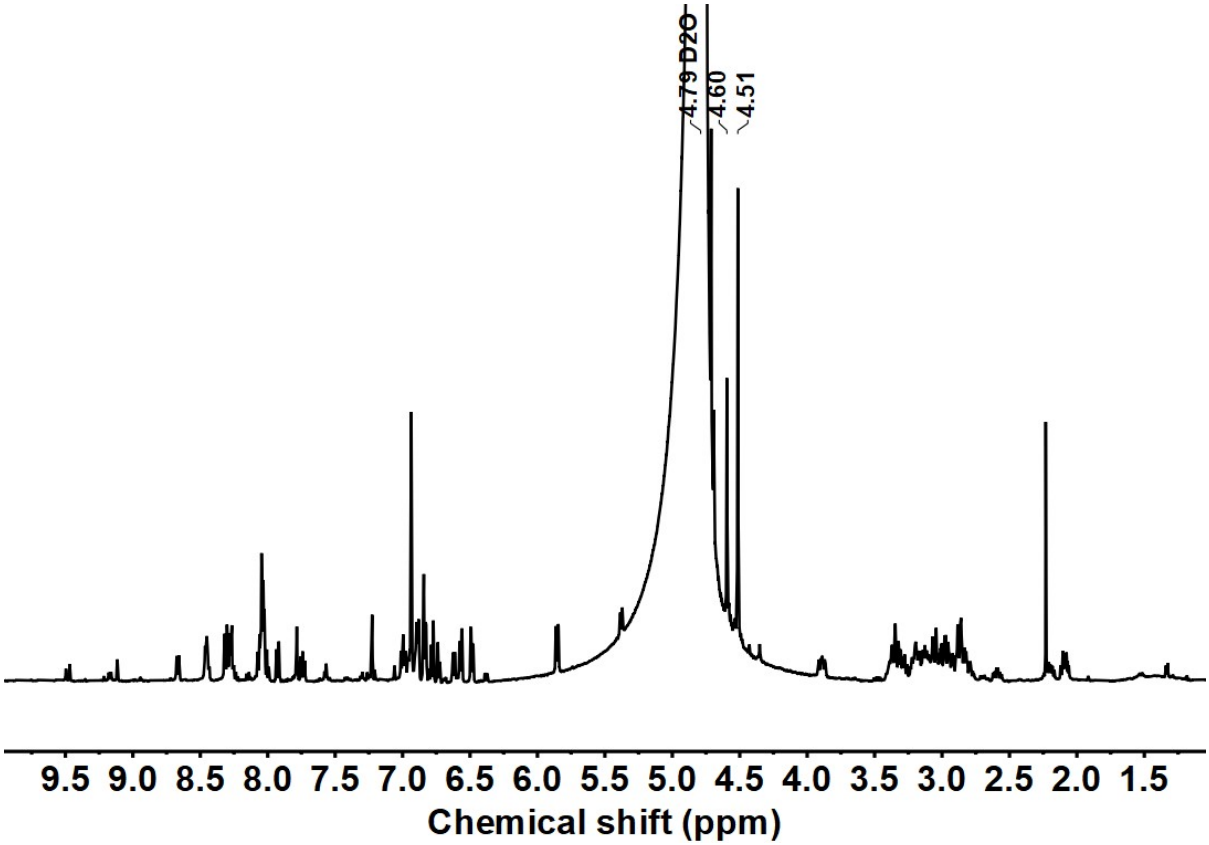

Figure S9. ^{1}H NMR spectra of **1** after photolysis, 500 MHz, D_2O.

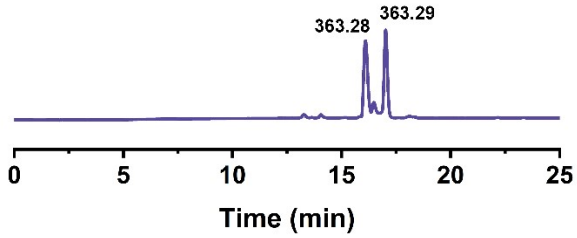

Figure S10. LC spectra of **1** after photolysis

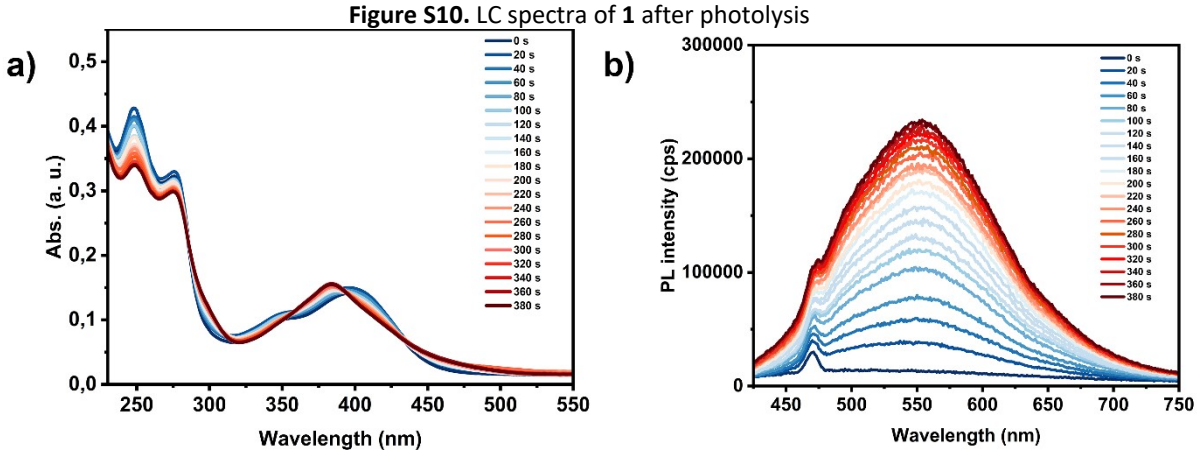

Figure S11. a) UV and b) Emission (λ_{exc}= 405 nm) spectra of photolysis of **1** (0.5 mM) after different reaction times in Milli Q water at 25 °C. The reaction mixture was diluted with Milli Q water to 2×10^{-4} M for UV and emission measurements.

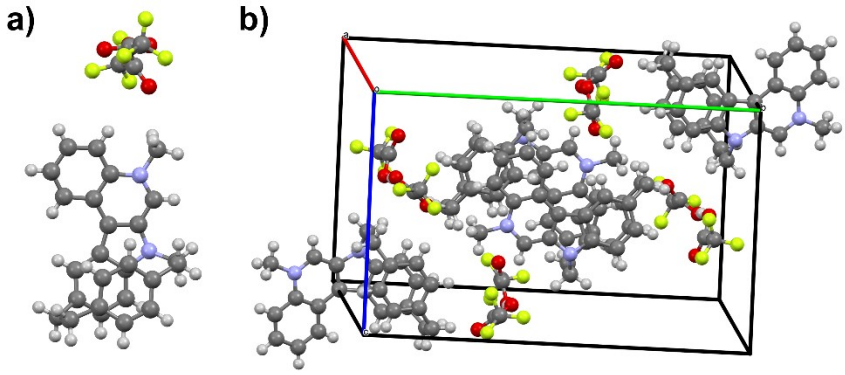

Figure S12. Crystal structure of a) **2**•$C_4HF_6O_4$; b) **2**•$C_4HF_6O_4$ in packing model.

Table S1 Crystal data and structure refinement for **2**•$C_4HF_6O_4$.

Identification code	**2**•$C_4HF_6O_4$
Empirical formula	$C_{30}H_{24}F_6N_2O_4$
Formula weight	590.51
Temperature/K	180
Crystal system	monoclinic
Space group	$P2_1/c$
a/Å	10.4972(3)
b/Å	20.6410(5)
c/Å	12.7749(4)
α/°	90
β/°	106.847(2)
γ/°	90
Volume/Å^3	2649.18(13)
Z	4
ρ_{calc}g/cm^3	1.481
μ/mm^{-1}	0.699
F(000)	1216.0
Crystal size/mm^3	0.14 × 0.12 × 0.03
Radiation	Ga Kα (λ = 1.34143)
2Θ range for data collection/°	9.176 to 114.992
Index ranges	-7 ≤ h ≤ 13, -25 ≤ k ≤ 25, -16 ≤ l ≤ 13
Reflections collected	34124
Independent reflections	5479 [R_{int} = 0.0374, R_{sigma} = 0.0344]
Independent reflections with I≥2σ (I)	3478
Data/restraints/parameters	5479/0/384
Goodness-of-fit on F^2	1.081
Final R indexes [I≥2σ (I)]	R_1 = 0.0534, wR_2 = 0.1567
Final R indexes [all data]	R_1 = 0.0804, wR_2 = 0.1665
Largest diff. peak/hole / e Å^{-3}	0.51/-0.61
CCDC number	2377054

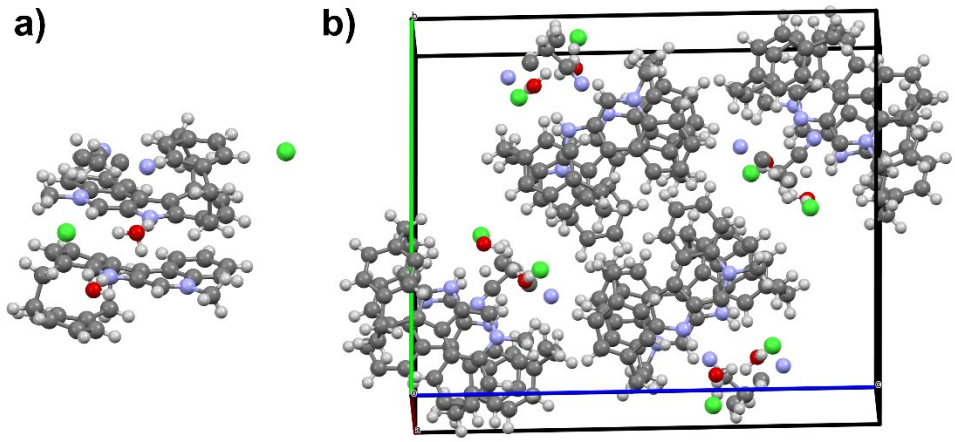

Figure S13. Crystal structure of a)2×(**3**•H_2O•½CH_3CN); b) 2×(**3**•H_2O•½CH_3CN) in packing model.

Table S2 Crystal data and structure refinement for 2×(**3**•H_2O•½CH_3CN).

Identification code	2×(**3**•H_2O•½CH_3CN)
Empirical formula	$C_{27}H_{26.5}ClN_{2.5}O$
Formula weight	437.46
Temperature/K	180
Crystal system	monoclinic
Space group	$P2_1/c$
a/Å	10.0721(3)
b/Å	19.0557(5)
c/Å	23.2446(8)
α/°	90
β/°	94.802(3)
γ/°	90
Volume/Å^3	4445.7(2)
Z	8
ρ_{calc}g/cm^3	1.307
μ/mm^{-1}	1.114
F(000)	1848.0
Crystal size/mm^3	0.12 × 0.04 × 0.03
Radiation	Ga Kα (λ = 1.34143)
2Θ range for data collection/°	6.64 to 124.998
Index ranges	-4 ≤ h ≤ 13, -25 ≤ k ≤ 25, -30 ≤ l ≤ 30
Reflections collected	54227
Independent reflections	10646 [R_{int} = 0.0330, R_{sigma} = 0.0355]
Independent reflections with I≥2σ (I)	7147
Data/restraints/parameters	10646/2/575
Goodness-of-fit on F^2	1.083
Final R indexes [I≥2σ (I)]	R_1 = 0.0587, wR_2 = 0.1777
Final R indexes [all data]	R_1 = 0.0814, wR_2 = 0.1883
Largest diff. peak/hole / e Å^{-3}	1.92/-0.54
CCDC number	2377055

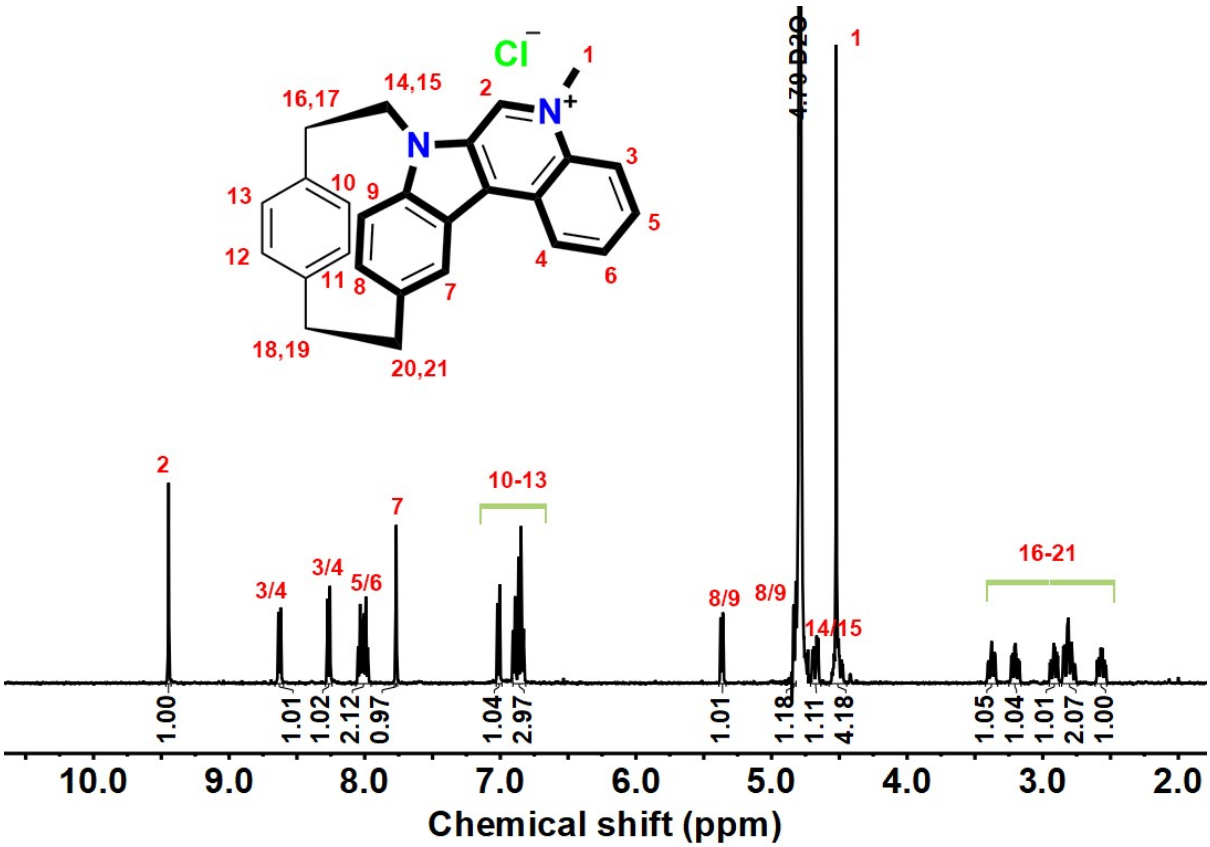

Figure S14. ^{1}H NMR spectra of **2**, 500 MHz, D_2O.

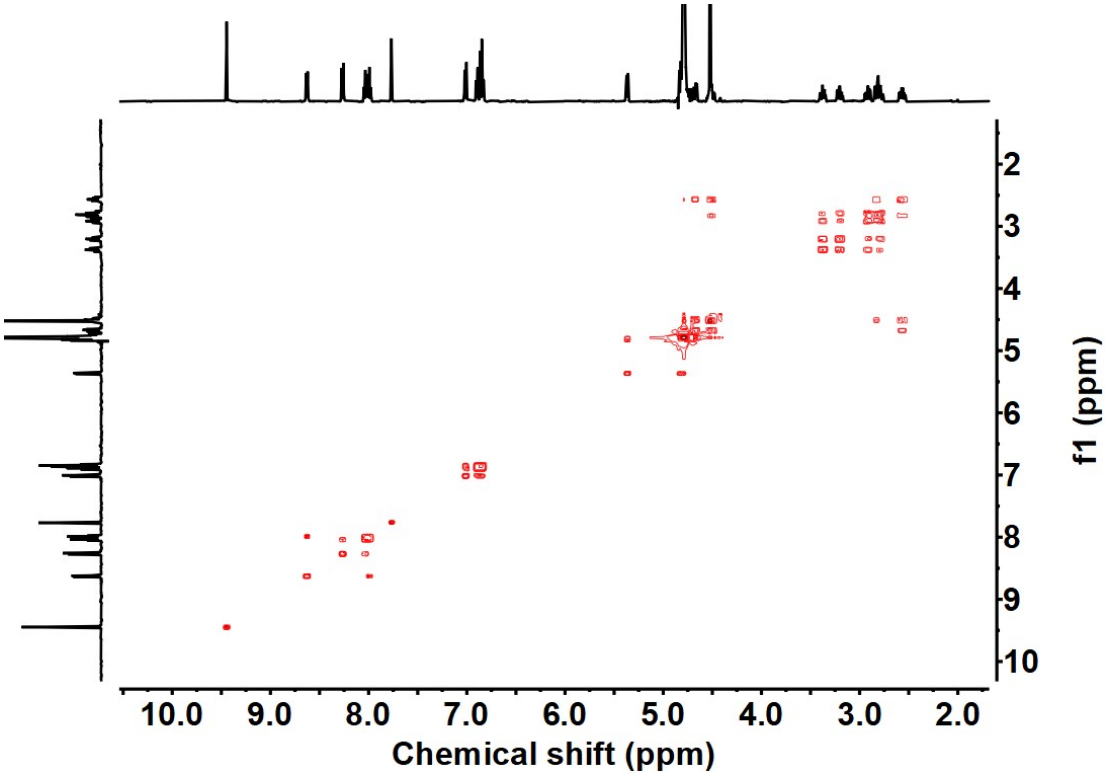

Figure S15. ^{1}H-^{1}H COSY spectra of **2**, D_2O.

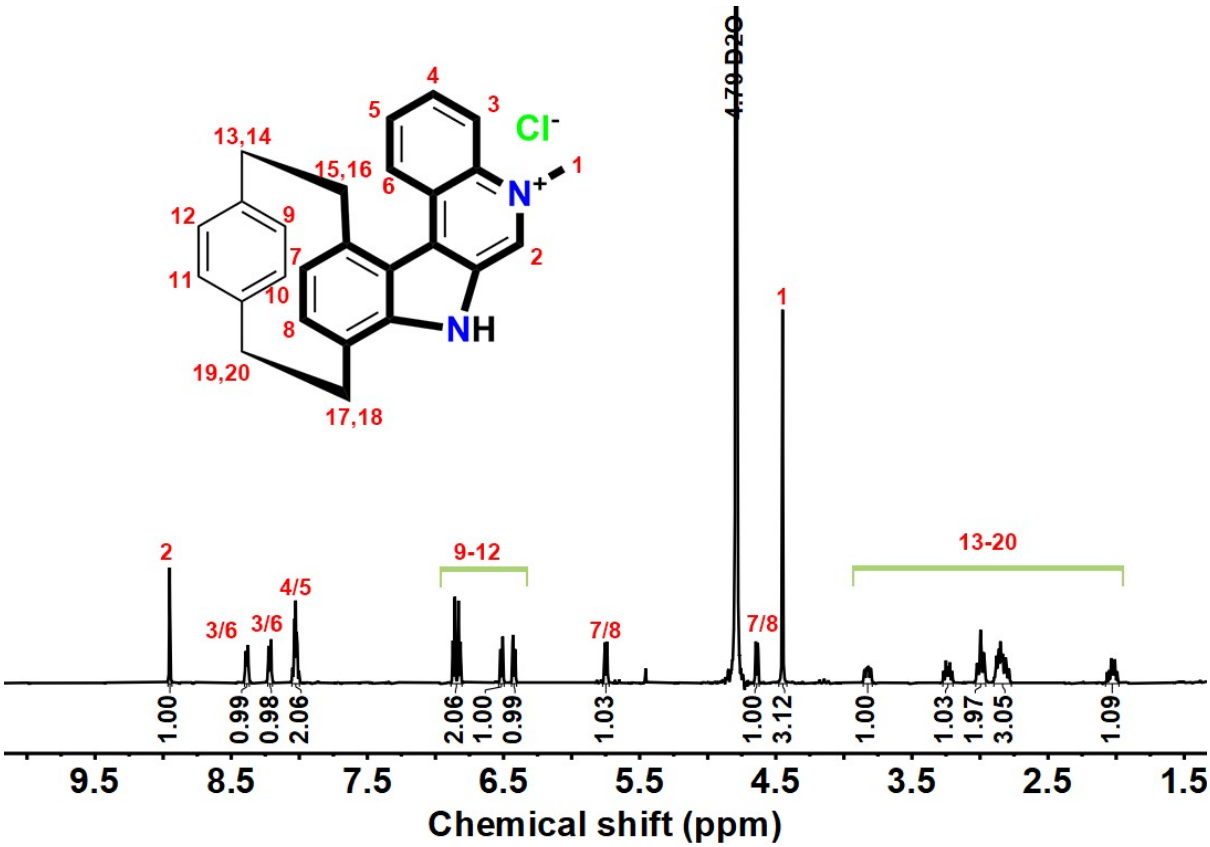

Figure S16. ^{1}H NMR spectra of **3**, 500 MHz, D_2O.

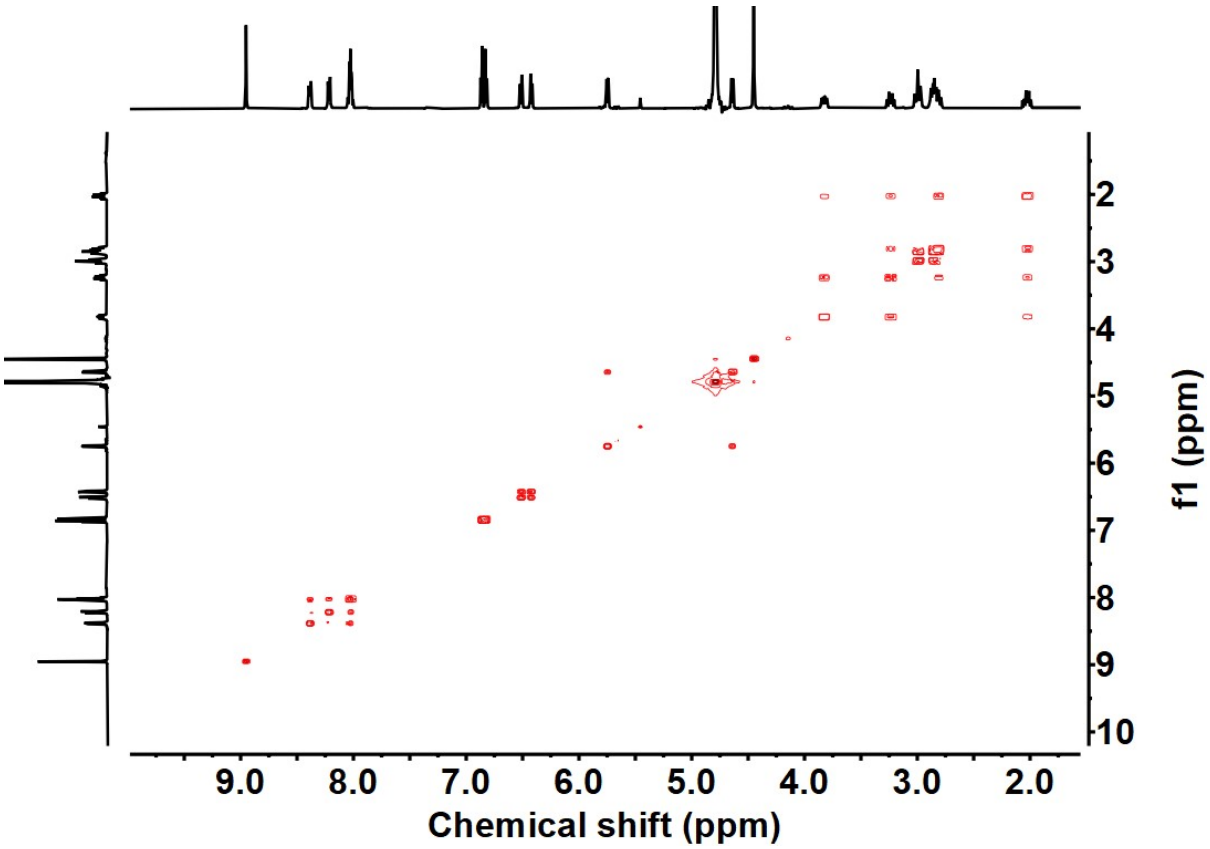

Figure S17. ^{1}H-^{1}H COSY spectra of **3**, D_2O.

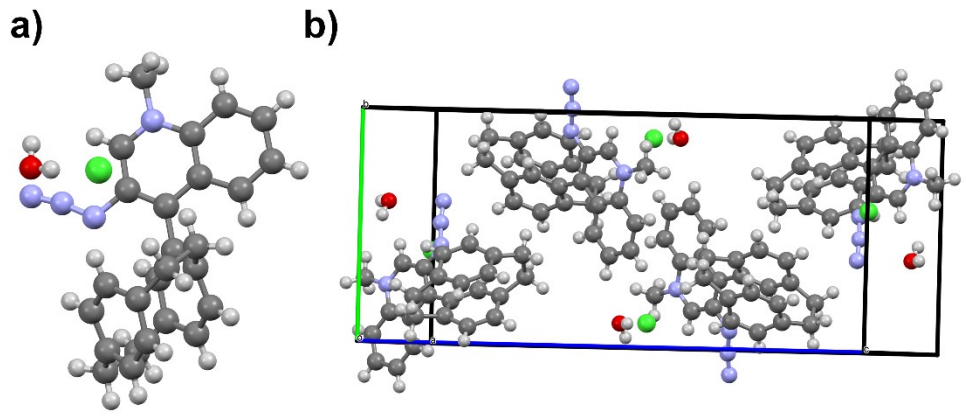

Figure S18. Crystal structure of a)**1**•H_2O; b) **1**•H_2O in packing model.

Table S3 Crystal data and structure refinement for **1**•H_2O.

Identification code	**1**•H_2O
Empirical formula	$C_{26}H_{25}ClN_4O$
Formula weight	444.95
Temperature/K	180
Crystal system	monoclinic
Space group	$P2_1/n$
a/Å	7.6248(2)
b/Å	10.9476(2)
c/Å	26.8702(7)
α/°	90
β/°	90.753(2)
γ/°	90
Volume/Å^3	2242.75(9)
Z	4
ρ_{calc}g/cm^3	1.318
μ/mm^{-1}	1.123
F(000)	936.0
Crystal size/mm^3	0.1 × 0.08 × 0.06
Radiation	Ga Kα (λ = 1.34143)
2Θ range for data collection/°	7.586 to 128
Index ranges	-6 ≤ h ≤ 10, -14 ≤ k ≤ 14, -31 ≤ l ≤ 35
Reflections collected	19114
Independent reflections	5457 [R_{int} = 0.0159, R_{sigma} = 0.0128]
Independent reflections with I≥2σ (I)	4797
Data/restraints/parameters	5457/0/293
Goodness-of-fit on F^2	1.063
Final R indexes [I≥2σ (I)]	R_1 = 0.0418, wR_2 = 0.1236
Final R indexes [all data]	R_1 = 0.0463, wR_2 = 0.1266
Largest diff. peak/hole / e Å^{-3}	0.72/-0.42
CCDC number	2377053

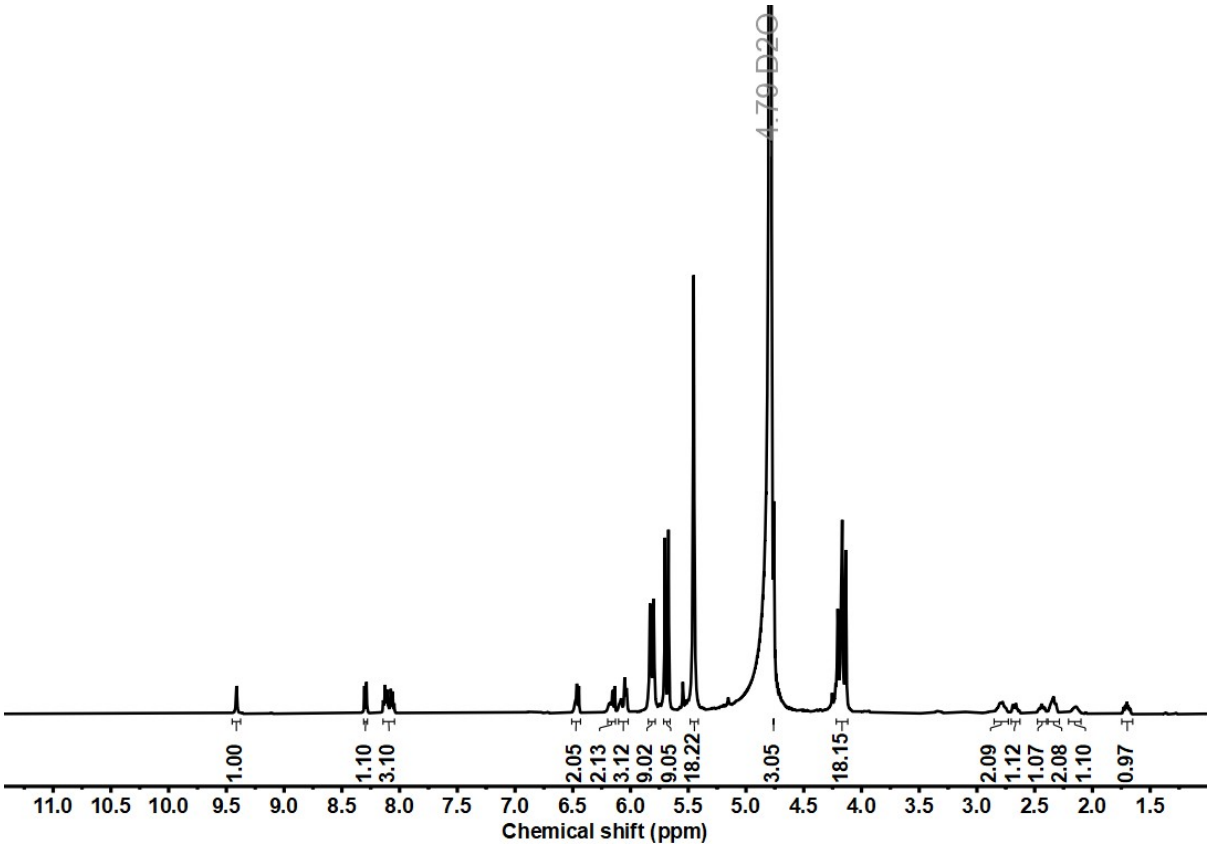

Figure S19. ^{1}H NMR spectra of **1**•CB8 (1:1) in 0.5mM, 500 MHz, D_2O.

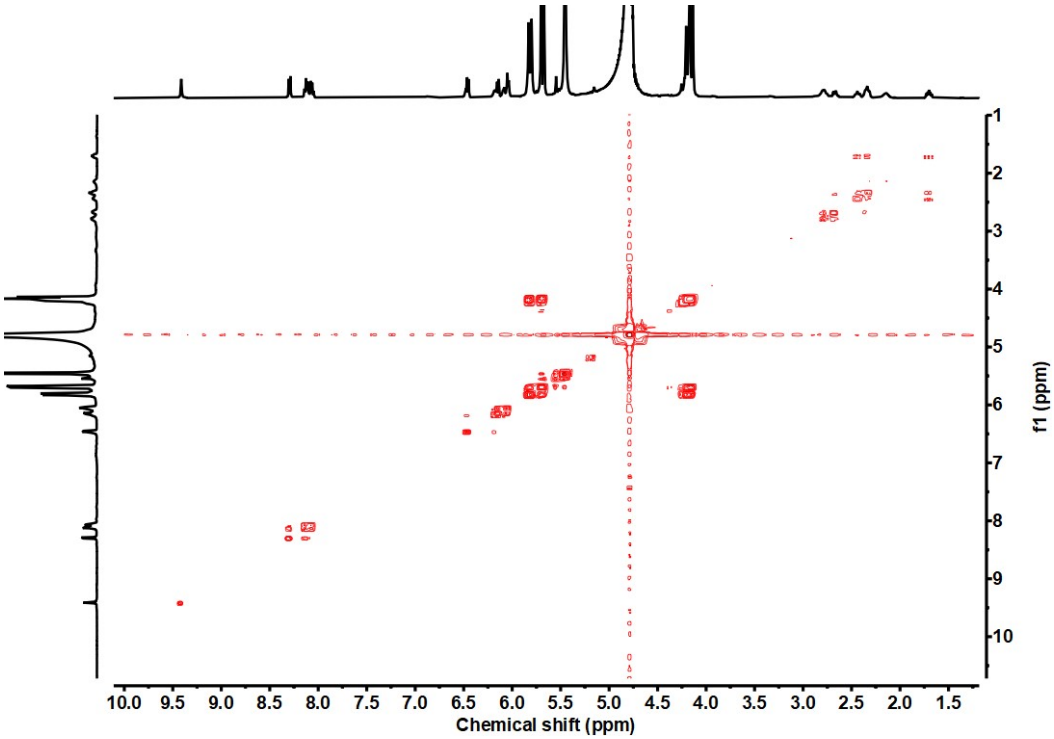

Figure S20. ^{1}H-^{1}H COSY spectra of **1**•CB8 (1:1) in 0.5mM, D_2O.

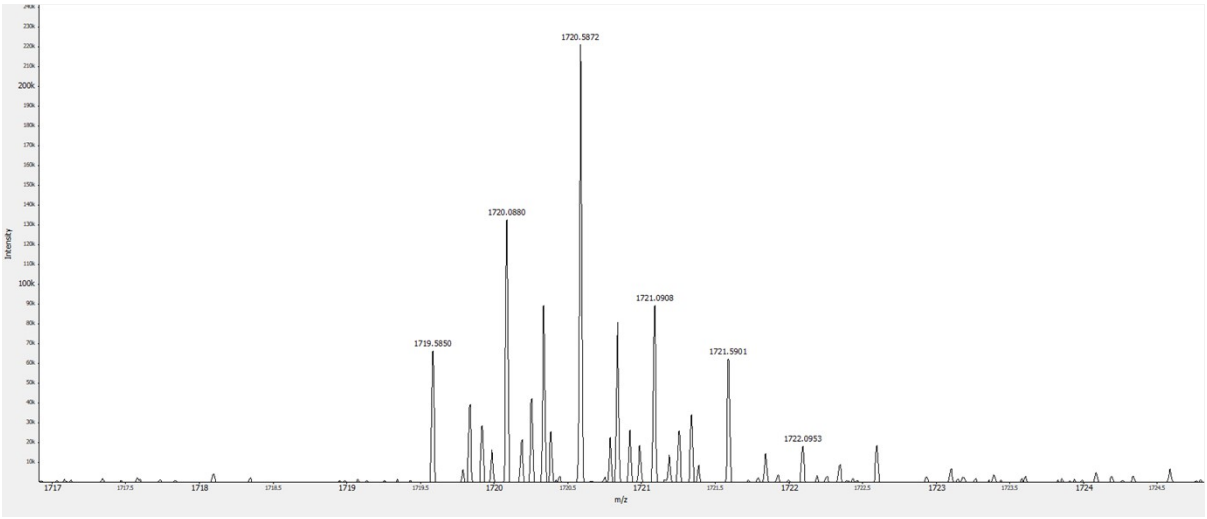

Figure S21. . ESI-MS spectra of aryl azide **1**+CB8 in 1:1 molar ratio in Milli Q water.

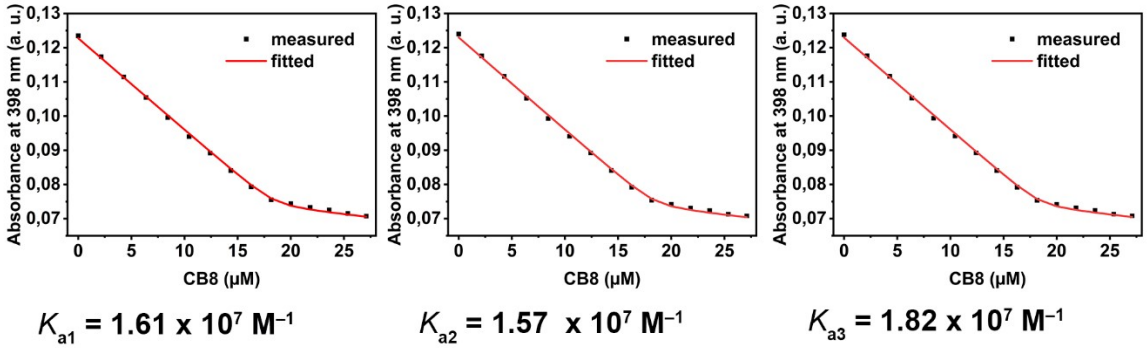

Average K_a = (1.67 ± 0.13) x 10^7 M^{-1}

Figure S22. UV absorbance changes of **1** at 398 nm upon increasing concentration of CB8 in Milli Q water. The binding constant value was determined by a non-linear curve fitting. The black squares depict the acquired data. The fit according to a 1:1 binding model is shown as red line. The error was calculated from 3 replica experiments as the standard deviation.

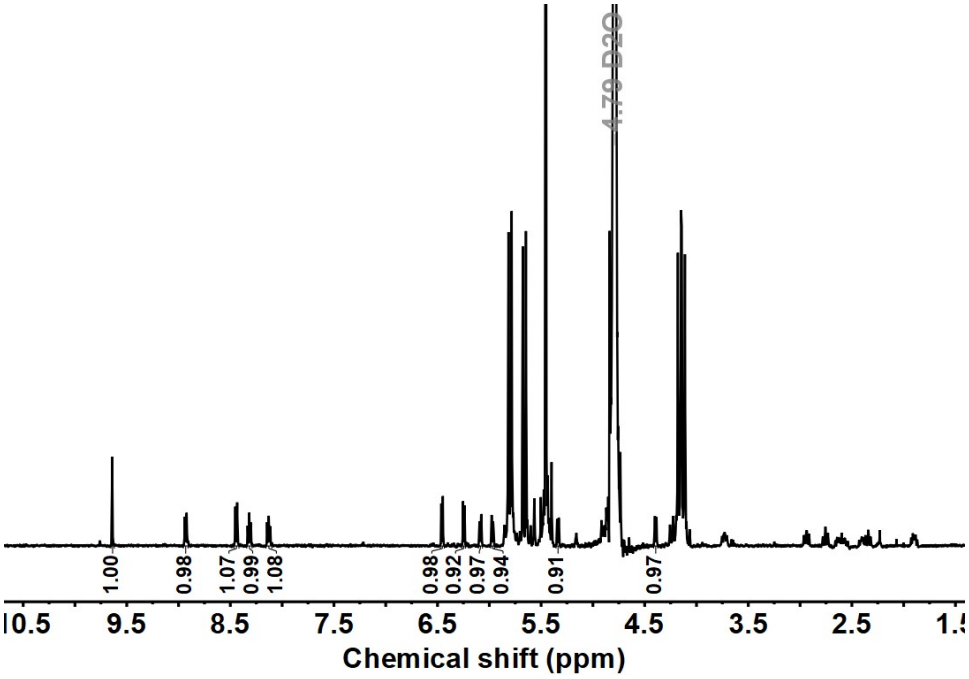

Figure S23. ^{1}H NMR spectra of **3**•CB8 (1:1, 0.5mM), 500 MHz, D_2O.

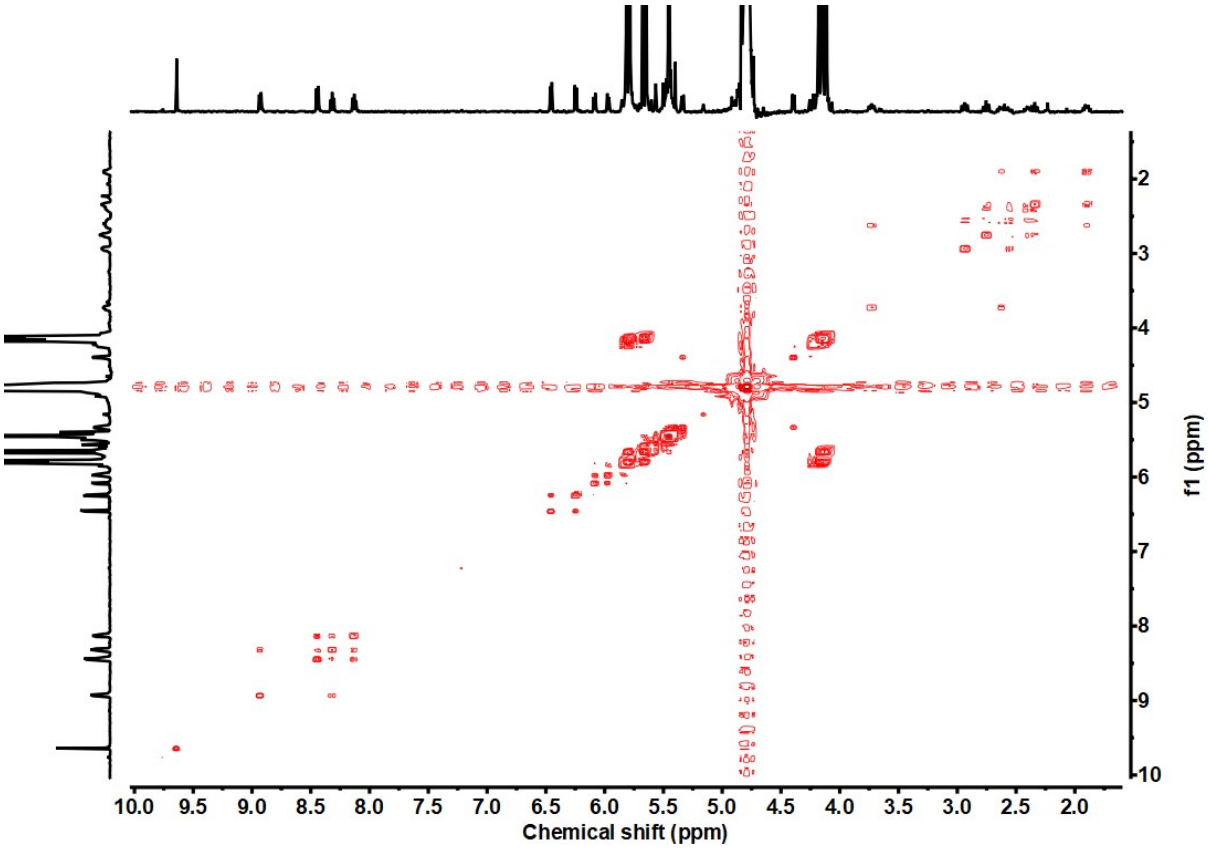

Figure S24. ^{1}H-^{1}H COSY spectra of **3**•CB8 (1:1) in 0.5mM, D_2O.

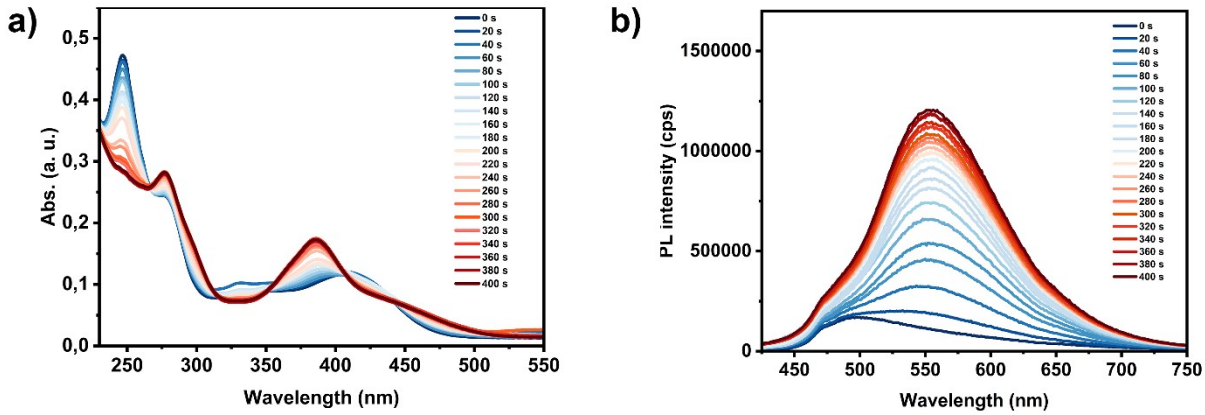

Figure S25. a) UV and b) Emission (λ_{exc}= 405 nm) spectra of photolysis of **1**•CB8 (1:1) (0.5 mM) after different reaction times in Milli Q water at 25 °C. The reaction mixture was diluted with Milli Q water to 2×10^{-4} M for UV and emission measurements.

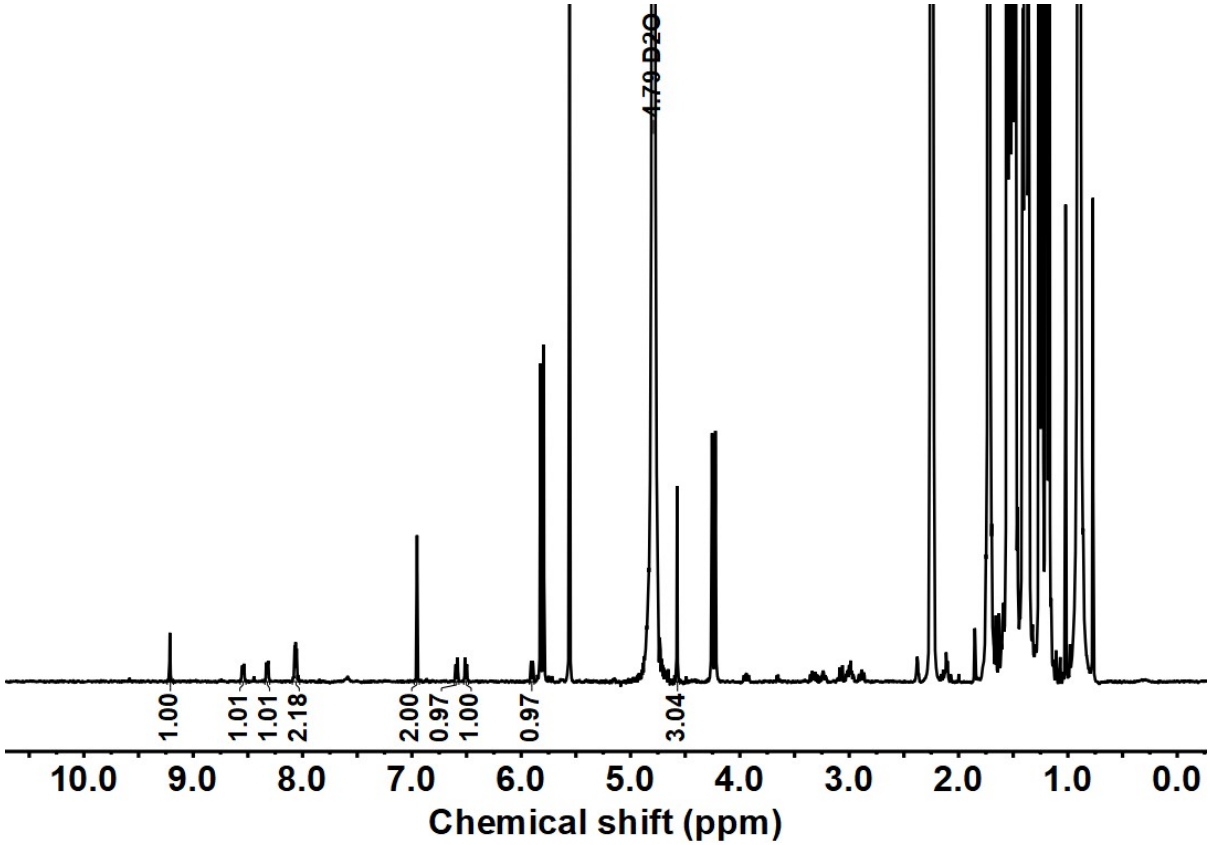

Figure S26. ^{1}H NMR spectra of **3**•CB8 (1:1, 0.5mM) with over amount of memantine, 500 MHz, D_2O.

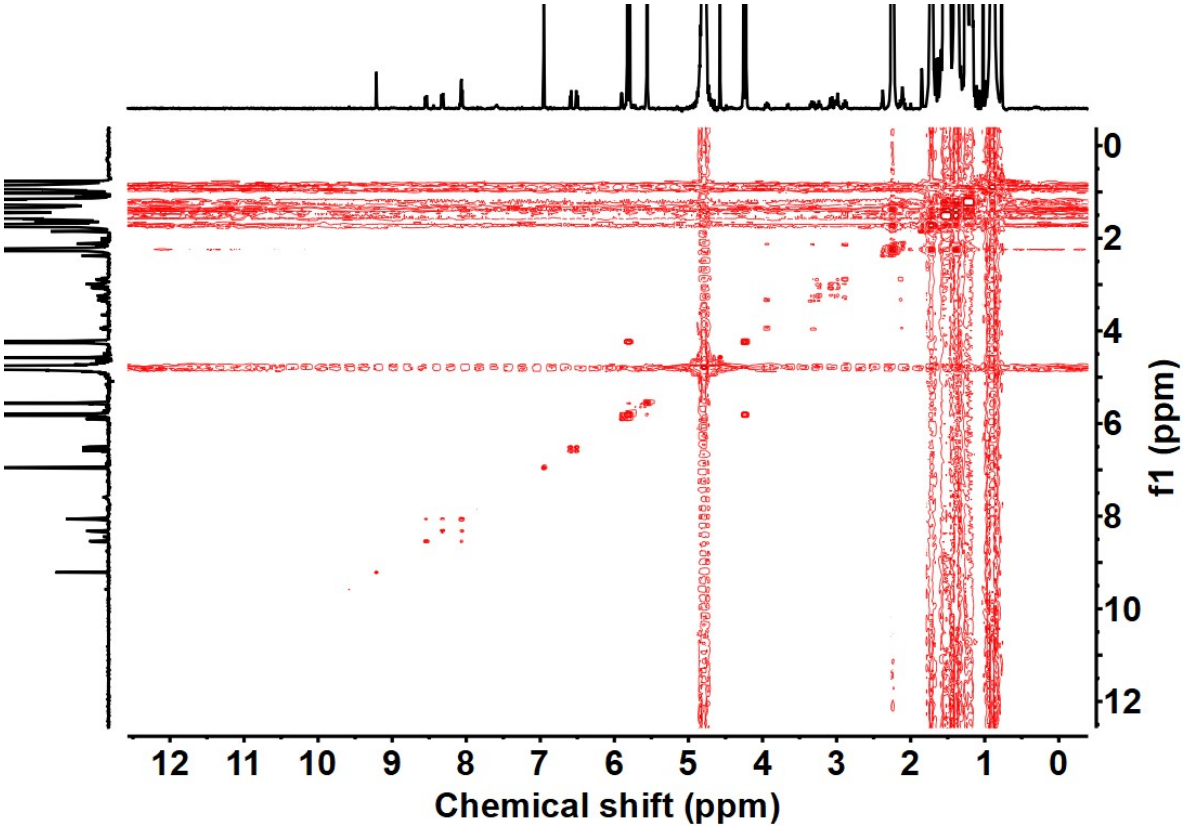

Figure S27. ^{1}H-^{1}H COSY spectra of **3**•CB8 (1:1, 0.5mM) with over amount of memantine, D_2O.

4. Competitive binding assay for binding constant determination

The binding constant determination using the method which was reported in the literature.[11] The method was based on the competitive binding assay (CBA), in which amantadine (Am) was utilized as a competitive guest whose binding constant with cucurbit[8]uril $K_{CB8\cdot Am}$= (8.19 ± 1.75) × 10^8 M^{-1} has reported.[12]

$$K_{rel} = \frac{[CB8\bullet 3][3]_{free}}{[CB8\bullet Am][Am]_{free}} \quad \text{Eq.1}$$

$[CB8]_{Total}$ = 0.4891 mM = [CB8•**3**] + [CB8•Am] Eq.2

$[Mem]_{Total}$ = 4.995 mM = $[Am]_{free}$ + [CB8•Am] Eq.3

$[\mathbf{3}]_{Total}$ = 0.6517 mM = $[\mathbf{3}]_{free}$ +[CB8•**3**] Eq.4

The interaction of **3** and amantadine with cucurbit[8]uril K_{rel} was determined by equation 1. The equilibrium of CB[8] (0.4891 mM), Am (4.995 mM), and **3** were attained in the D_2O for 48h at 298 K, where two similar proportions peaks with 5.53 ppm [CB8•Am] and 5.44 ppm [CB8•**3**] chemical shift in NMR spectra were observed. The relative concentration of [CB8·**3**] was calculated as 0.3132 mM by integrating the relative resonances in the NMR spectra. Then equation 2 allows us to calculate the [CB8•Am] as 0.1759 mM, which was substituted in equation 3 to calculate $[Am]_{free}$ as 4.8191 mM. With the same method, $[\mathbf{3}]_{free}$ was calculated as 0.3385 mM using equation 4.

The K_{rel} value was calculated by substitution of [CB8•**3**], $[\mathbf{3}]_{free}$, [CB8•Am], and $[Am]_{free}$ into equation 1, which was obtained as 0.1251. Substitution of $K_{CB8•Am} = (8.19 \pm 1.75) \times 10^8\ M^{-1}$ and K_{rel} in equation 5 to obtain $K_{CB8•\mathbf{3}} = 1.02 \times 10^8\ M^{-1}$ (equation 6). The uncertainty of $\sigma K_{CB8•\mathbf{3}}$ can be calculated by equation 7, where $\sigma(K_{CB8•Am})/\ \sigma K_{CB8•Am} = 0.1006$ and $\sigma(K_{rel})/\ \sigma K_{rel} = 0.10$ [Note that we are using the even more conservative 10% error in this analysis] to give the percent error in $K_{CB8•\mathbf{3}}$ equation 8. Substituting equation 6 into equation 9 gives $\sigma K_{CB8•\mathbf{3}}$ as $0.14 \times 10^8 M^{-1}$, which was finally combined into equation 10 to give the final binding constant $K_{CB8•\mathbf{3}} = (1.02 \pm 0.14) \times 10^8 M^{-1}$.

$$K_{CB8•\mathbf{3}} = (K_{CB8•Mem})(K_{rel}) \qquad \text{Eq.5}$$

$$K_{CB8•\mathbf{3}} = 1.02 \times 10^8 M^{-1} \qquad \text{Eq.6}$$

$$\left(\frac{\sigma K_{CB8•3}}{K_{CB8•3}}\right)^2 = \left(\frac{\sigma K_{CB8•Am}}{K_{CB8•Am}}\right)^2 + \left(\frac{\sigma K_{rel}}{K_{rel}}\right)^2 \qquad \text{Eq.7}$$

$$\frac{\sigma K_{CB8•3}}{K_{CB8•3}} = 0.1418\ (14.18\%) \qquad \text{Eq.8}$$

$$\sigma K_{CB8•3} = 0.1418 \times (1.02 \times 10^8 M^{-1}) = 0.14 \times 10^8 M^{-1} \qquad \text{Eq.9}$$

$$K_{CB8•\mathbf{3}} = (1.02 \pm 0.14) \times 10^8 M^{-1}. \qquad \text{Eq.10}$$

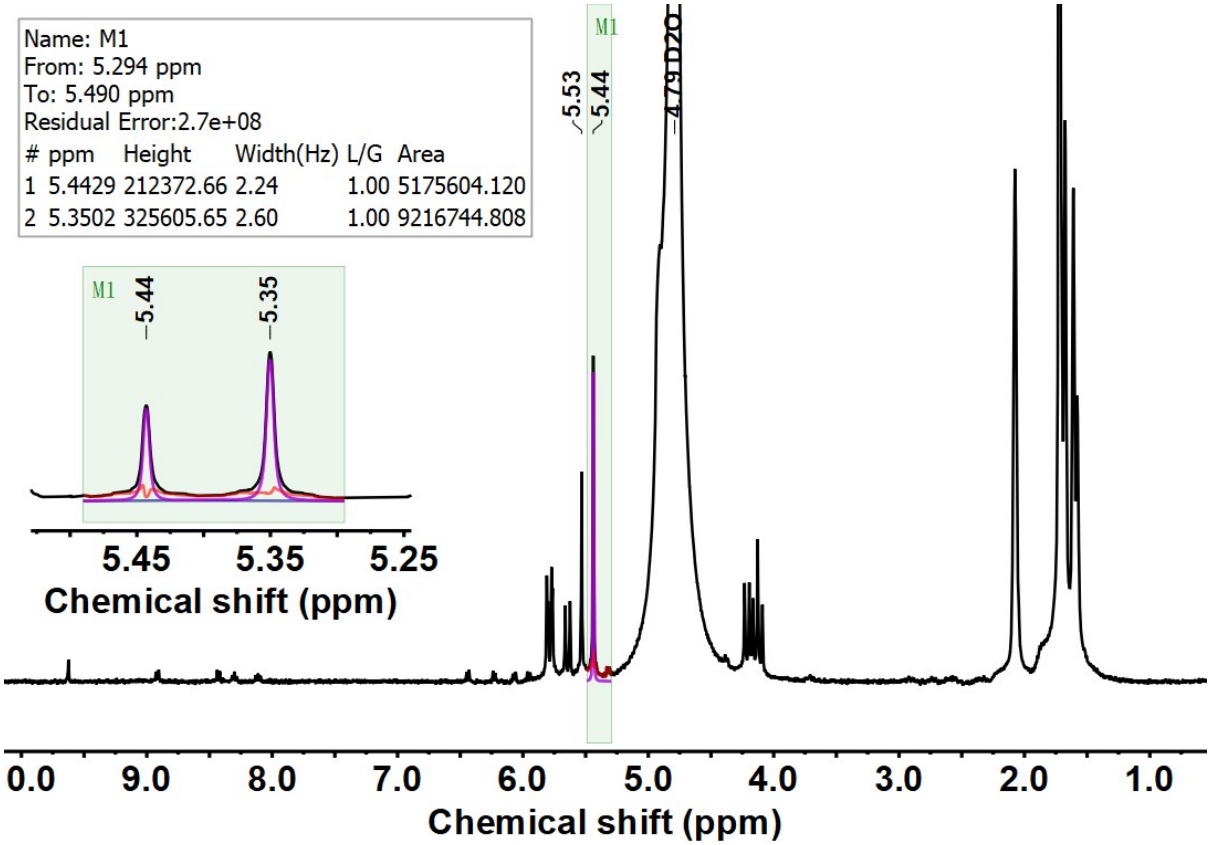

Figure S28. ^{1}H NMR spectra were used in the competitive binding assay determination of K_{rel} value for [CB8•**3**] and [CB8•Am]. $[CB8]_{Total}$ = 0.4891 mM, $[Am]_{Total}$ = 4.995 mM, $[\mathbf{3}]_{Total}$ = 0.6517 mM, 500 MHz, D_2O

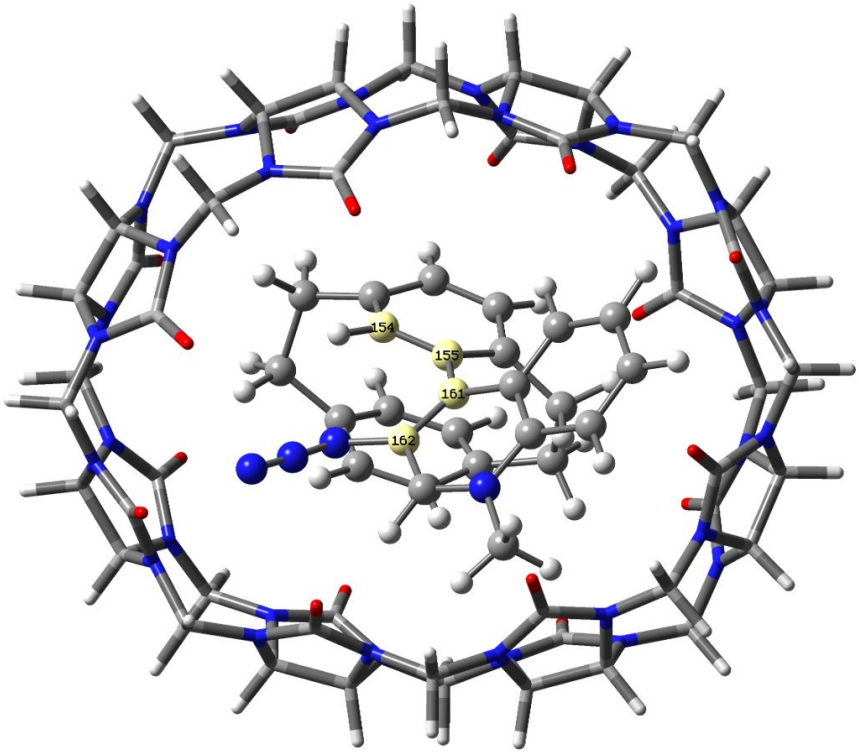

Figure S29. Energy minimized **1**●CB8 complex at 6-31G(d,p)/B3LYP/GD3.

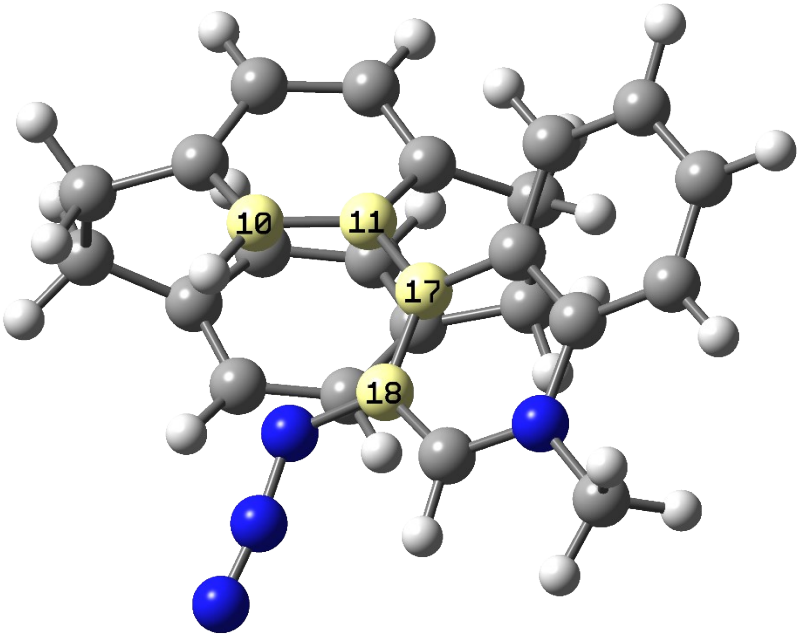

Figure S30. Starting geometry of **1** at 6-31G(d,p)/B3LYP/GD3.

5. References

1. Dolomanov, O.V., Bourhis, L.J., Gildea, R.J, Howard, J.A.K. & Puschmann, H. (2009), J. Appl. Cryst. 42, 339-341.
2. Sheldrick, G.M. (2015), Acta Cryst. A71, 3-8.
3. Sheldrick, G.M. (2015), Acta Cryst. C71, 3-8.
4. Hariharan, P. C., & Pople, J. A. (1974), Molecular Physics, 27(1), 209–214.
5. G. A. Petersson, A. Bennett, T. G. Tensfeldt, M. A. Al‐Laham, W. A. Shirley, J. Mantzaris, J. Chem. Phys. 1988, 89 (4), 2193–2218.
6. S. Grimme, J. Antony, S. Ehrlich, H. Krieg, J. Chem. Phys., 2010, 132 (15), 154104.
7. G. W. T. M. J. Frisch, H. B. Schlegel, G. E. Scuseria, M. A. Robb, J. R. Cheeseman, G. Scalmani, V. Barone, B. Mennucci, G. A. Petersson, H. Nakatsuji, M. Caricato, X. Li, H. P. Hratchian, A. F. Izmaylov, J. Bloino, G. Zheng, J. L. Sonnenberg, M. Hada, M. Ehara, K. Toyota, R. Fukuda, J. Hasegawa, M. Ishida, T. Nakajima, Y. Honda, O. Kitao, H. Nakai, T. Vreven, J. A. Montgomery Jr., J. E. Peralta, F. Ogliaro, M. Bearpark, J. J. Heyd, E. Brothers, K. N. Kudin, V. N. Staroverov, R. Kobayashi, J. Normand, K. Raghavachari, A. Rendell, J. C. Burant, S. S. Iyengar, J. Tomasi, M. Cossi, N. Rega, J. M. Millam, M. Klene, J. E. Knox, J. B. Cross, V. Bakken, C. Adamo, J. Jaramillo, R. Gomperts, R. E. Stratmann, O. Yazyev, A. J. Austin, R. Cammi, C. Pomelli, J. W. Ochterski, R. L. Martin, K. Morokuma, V. G. Zakrzewski, G. A. Voth, P. Salvador, J. J. Dannenberg, S. Dapprich, A. D. Daniels, Ö. Farkas, J. B. Foresman, J. V. Ortiz, J. Cioslowski, D. J. Fox, , Gaussian Inc., Gaussian 16 rev.C.01 Wallingford, CT, 2019.
8. X. Qiu, E. Pohl, Q. Cai, J. Seibert, Y. Li, S. Leopold, O. Fuhr, M. A. R. Meier, U. Schepers, S. Bräse, Adv. Funct. Mater. 2024, 2401938.
9. D. M. Knoll and S. Bräse, ACS Omega. 2018, 3, 9, 12158–12162.
10. L. Noël-Duchesneau, J. Maddaluno, M. Durandetti, ChemCatChem 2019, 11, 4154.
11. D. Sigwalt, M. Šekutor, L. Cao, P. Y. Zavalij, J. Hostaš, H. Ajani, P. Hobza, K. Mlinarić-Majerski, R. Glaser, L. Isaacs, J. Am. Chem. Soc. 2017, 139, 8, 3249–3258.
12. S. Liu,C. Ruspic, P. Mukhopadhyay, S. Chakrabarti, P. Y. Zavalij, L. Isaacs, J. Am. Chem. Soc. 2005, 127, 45, 15959–15967